Mitochondrial respiratory states and rates:
Building blocks of mitochondrial physiology
Part 1.

MitoEAGLE Network

Corresponding author: Gnaiger E

Contributing co-authors

Acuna-Castroviejo D, Ahn B, Alves MG, Amati F, Aral C, Arandarčikaitė O, Åsander Frostner E, Bailey DM, Bastos Sant'Anna Silva AC, Battino M, Beard DA, Ben-Shachar D, Bishop D, Borutaitė V, Breton S, Brown GC, Brown RA, Buettner GR, Burtscher J, Calabria E, Cardoso LHD, Carvalho E, Casado Pinna M, Cervinkova Z, Chang SC, Chen Q, Chicco AJ, Chinopoulos C, Coen PM, Collins JL, Crisóstomo L, Davis MS, Dias T, Distefano G, Doerrier C, Drahota Z, Duchen MR, Ehinger J, Elmer E, Endlicher R, Fell DA, Ferko M, Ferreira JCB, Filipovska A, Fisar Z, Fisher J, Garcia-Roves PM, Garcia-Souza LF, Genova ML, Gonzalo H, Goodpaster BH, Gorr TA, Grefte S, Han J, Harrison DK, Hellgren KT, Hernansanz P, Holland O, Hoppel CL, Houstek J, Hunger M, Iglesias-Gonzalez J, Irving BA, Iyer S, Jackson CB, Jadiya P, Jansen-Dürr P, Jespersen NR, Jha RK, Kaambre T, Kane DA, Kappler L, Karabatsiakis A, Keijer J, Keppner G, Komlodi T, Kopitar-Jerala N, Krako Jakovljevic N, Kuang J, Kucera O, Labieniec-Watala M, Lai N, Laner V, Larsen TS, Lee HK, Lemieux H, Lerfall J, Lucchinetti E, MacMillan-Crow LA, Makrecka-Kuka M, Meszaros AT, Michalak S, Moisoi N, Molina AJA, Montaigne D, Moore AL, Moreira BP, Mracek T, Muntane J, Muntean DM, Murray AJ, Nedergaard J, Nemec M, Newsom S, Nozickova K, O'Gorman D, Oliveira PF, Oliveira PJ, Orynbayeva Z, Pak YK, Palmeira CM, Patel HH, Pecina P, Pereira da Silva Grilo da Silva F, Pesta D, Petit PX, Pichaud N, Pirkmajer S, Porter RK, Pranger F, Prochownik EV, Puurand M, Radenkovic F, Reboredo P, Renner-Sattler K, Robinson MM, Rohlena J, Røsland GV, Rossiter HB, Rybacka-Mossakowska J, Saada A, Salvadego D, Scatena R, Schartner M, Scheibye-Knudsen M, Schilling JM, Schlattner U, Schoenfeld P, Schwarzer C, Scott GR, Shabalina IG, Sharma P, Shevchuk I, Siewiera K, Singer D, Sobotka O, Sokolova I, Spinazzi M, Stankova P, Stier A, Stocker R, Sumbalova Z, Suravajhala P, Tanaka M, Tandler B, Tepp K, Tomar D, Towheed A, Tretter L, Trivigno C, Tronstad KJ, Trougakos IP, Tyrrell DJ, Urban T, Valentine JM, Velika B, Vendelin M, Vercesi AE, Victor VM, Villena JA, Wagner BA, Ward ML, Watala C, Wei YH, Wieckowski MR, Wohlwend M, Wolff J, Wuest RCI, Zaugg K, Zaugg M, Zorzano A

Supporting co-authors:

Bakker BM, Bernardi P, Boetker HE, Borsheim E, Bouitbir J, Calbet JA, Calzia E, Chaurasia B, Clementi E, Coker RH, Collin A, Das AM, De Palma C, Dubouchaud H, Durham WJ, Dyrstad SE, Engin AB, Fischer M, Fornaro M, Gan Z, Garlid KD, Garten A, Gourlay CW, Granata C, Haas CB, Haavik J, Haendeler J, Hand SC, Hepple RT, Hickey AJ, Hoel F, Jang DH, Kainulainen H, Khamoui AV, Klingenspor M, Koopman WJH, Kowaltowski AJ, Krajcova A, Lane N, Lenaz G, Liu J, Liu SS, Malik A, Markova M, Mazat JP, Menze MA, Methner A, Neuzil J, Oliveira MT, Pallotta ML, Parajuli N, Pettersen IKN, Porter C, Pulinilkunnil T, Ropelle ER, Salin K, Sandi C, Sazanov LA, Silber AM, Skolik R, Smenes BT, Soares FAA, Sonkar VK, Swerdlow RH, Szabo I, Trifunovic A, Thyfault JP, Vieyra A, Votion DM, Williams C, Zischka H

Updates and discussion:
http://www.mitoeagle.org/index.php/MitoEAGLE_preprint_2018-02-08
Correspondence: Gnaiger E
Chair COST Action CA15203 MitoEAGLE – http://www.mitoeagle.org
Department of Visceral, Transplant and Thoracic Surgery, D. Swarovski Research
Laboratory, Medical University of Innsbruck, Innrain 66/4, A-6020 Innsbruck, Austria
Email: erich.gnaiger@i-med.ac.at
Tel: +43 512 566796, Fax: +43 512 566796 20

Contents

Abstract As the knowledge base and importance of mitochondrial physiology to human health expand, the necessity for harmonizing nomenclature concerning mitochondrial respiratory states and rates has become increasingly apparent. Clarity of concept and consistency of nomenclature are key trademarks of a research field. These trademarks facilitate effective transdisciplinary communication, education, and ultimately further discovery. Peter Mitchell's chemiosmotic theory establishes the mechanism of energy transformation and coupling in oxidative phosphorylation. The unifying concept of the protonmotive force provides the framework for developing a consistent theory and nomenclature for mitochondrial physiology and bioenergetics. Herein, we follow IUPAC guidelines on general terms of physical chemistry, extended by considerations on open systems and irreversible thermodynamics. We align the nomenclature and symbols of classical bioenergetics with a concept-driven constructive terminology to express the meaning of each quantity clearly and consistently. In this position statement, in the frame of COST Action MitoEAGLE, we endeavour to provide a balanced view on mitochondrial respiratory control and a critical discussion on reporting data of mitochondrial respiration in terms of metabolic flows and fluxes. Uniform standards for evaluation of respiratory states and rates will ultimately support the development of databases of mitochondrial respiratory function in species, tissues, and cells.


Executive summary

1. In view of broad implications on health care, mitochondrial researchers face an increasing responsibility to disseminate their fundamental knowledge and novel discoveries to a wide range of stakeholders and scientists beyond the group of specialists. This requires implementation of a commonly accepted terminology within the discipline and standardization in the translational context. Authors, reviewers, journal editors, and lecturers are challenged to collaborate with the aim to harmonize the nomenclature in the growing field of mitochondrial physiology and bioenergetics.

2. Aerobic energy metabolism in mammalian mitochondria depends on the coupling of $ADP \rightarrow ATP$ phosphorylation to oxygen consumption in catabolic reactions. In this process of oxidative phosphorylation, coupling is mediated by translocation of protons through respiratory proton pumps operating across the inner mitochondrial membrane and generating or utilizing the protonmotive force measured between the mitochondrial matrix and intermembrane compartment. Compartmental coupling thus distinguishes vectorial oxidative phosphorylation from fermentation as the counterpart of cellular core energy metabolism.

3. To exclude fermentation and other cytosolic interactions from exerting an effect on mitochondrial metabolism, the barrier function of the plasma membrane must be disrupted. Selective removal or permeabilization of the plasma membrane yields mitochondrial preparations—including isolated mitochondria, tissue and cellular preparations—with structural and functional integrity. Then extra-mitochondrial concentrations of fuel substrates transported into the mitochondrial matrix, ADP, ATP, inorganic phosphate, and cations including H^+ can be controlled to determine mitochondrial function under a set of conditions defined as coupling control states.

A concept-driven terminology of bioenergetics incorporates in its terms and symbols explicitly information on the nature of respiratory states, that makes the technical terms readily recognized and easy to understand.
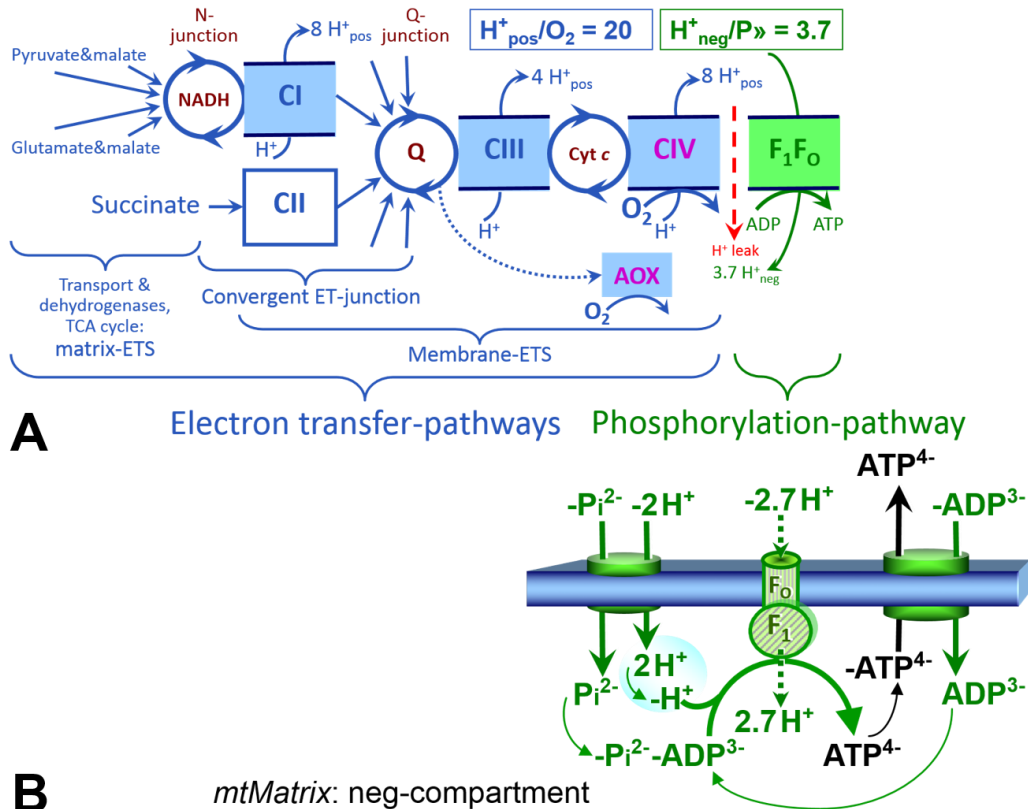
Fig. 1. The oxidative phosphorylation (OXPHOS) system. (A) The mitochondrial electron transfer system (ETS) is fuelled by diffusion and transport of substrates across the mtOM and mtIM and consists of the matrix-ETS and membrane-ETS. ET-pathways are coupled to the phosphorylation-pathway. ET-pathways converge at the N-junction and Q-junction. Additional arrows indicate electron entry into the Q-junction through electron transferring flavoprotein, glycerophosphate dehydrogenase, dihydro-orotate dehydrogenase, choline dehydrogenase, and sulfide-ubiquinone oxidoreductase. The dotted arrow indicates the branched pathway of oxygen consumption by alternative quinol oxidase (AOX). The H^+_{pos}/O_2 ratio is the outward proton flux from the matrix space to the positively (pos) charged compartment, divided by catabolic O_2 flux in the NADH-pathway. The $H^+_{neg}/P»$ ratio is the inward proton flux from the inter-membrane space to the negatively (neg) charged matrix space, divided by the flux of phosphorylation of ADP to ATP (Eq. 1). These are not fixed stoichiometries due to ion leaks and proton slip. **(B)** Phosphorylation-pathway catalyzed by the proton pump F_1F_O-ATPase (F-ATPase), adenine nucleotide translocase, and inorganic phosphate transporter. The $H^+_{neg}/P»$ stoichiometry is the sum of the coupling stoichiometry in the F-ATPase reaction (-2.7 H^+_{pos} from the positive intermembrane space, 2.7 H^+_{neg} to the matrix, *i.e.*, the negative compartment) and the proton balance in the translocation of ADP^{2-}, ATP^{3-} and P_i^{2-}. Modified from (A) Lemieux *et al.* (2017) and (B) Gnaiger (2014).

4. Mitochondrial coupling states are defined according to the control of respiratory oxygen consumption by the protonmotive force. Capacities of oxidative phosphorylation and electron transfer capacities are measured at kinetically saturating concentrations of fuel substrates, ADP and inorganic phosphate, or at optimal uncoupler concentrations, respectively. Respiratory capacities are a measure of the upper bound of the rates of respiration, providing reference values for the diagnosis of health and disease, and for evaluation of the effects of **E**volutionary background, **A**ge, **G**ender and sex, **L**ifestyle and **E**nvironment (EAGLE).

5. Some degree of uncoupling is a characteristic of energy-transformations across membranes. Uncoupling is caused by a variety of physiological, pathological, toxicological, pharmacological and environmental conditions that exert an influence not only on the proton leak and cation cycling, but also on proton slip within the proton pumps and the structural integrity of the mitochondria. A more loosely coupled state is induced by stimulation of mitochondrial superoxide formation and the bypass of proton pumps. In addition, uncoupling by application of protonophores represents an experimental intervention for the transition from a well-coupled to the noncoupled state of mitochondrial respiration.

6. Respiratory oxygen consumption rates have to be carefully normalized to enable meta-analytic studies beyond the specific question of a particular experiment. Therefore, all raw data should be published in a supplemental table or open access data repository. Normalization of rates for the volume of the experimental chamber (the measuring system) is distinguished from normalization for (*1*) the volume or mass of the experimental sample, (*2*) the number of objects (cells, organisms), and (*3*) the concentration of mitochondrial markers in the chamber.

7. The consistent use of terms and symbols discussed in this MitoEAGLE position statement will facilitate transdisciplinary communication and support further developments of a database on bioenergetics and mitochondrial physiology. The present considerations are focused on studies with mitochondrial preparations. These will be extended in a series of reports on pathway control of mitochondrial respiration, the protonmotive force, respiratory states in intact cells, and harmonization of experimental procedures.

Box 1: In brief – Mitochondria and Bioblasts

Mitochondria are the oxygen-consuming electrochemical generators evolved from endosymbiotic bacteria (Margulis 1970; Lane 2005). They were described by Richard Altmann (1894) as 'bioblasts', which include not only the mitochondria as presently defined, but also symbiotic and free-living bacteria. The word 'mitochondria' (Greek mitos: thread; chondros: granule) was introduced by Carl Benda (1898).

Mitochondrial dysfunction is associated with a wide variety of genetic and degenerative diseases. Robust mitochondrial function is supported by physical exercise and caloric balance, and is central for sustained metabolic health throughout life. Therefore, a more consistent presentation of mitochondrial physiology will improve our understanding of the etiology of disease, the diagnostic repertoire of mitochondrial medicine, with a focus on protective medicine, lifestyle and healthy aging.

We now recognize mitochondria as dynamic organelles with a double membrane that are contained within eukaryotic cells. The mitochondrial inner membrane (mtIM) shows dynamic tubular to disk-shaped cristae that separate the mitochondrial matrix, *i.e.*, the negatively charged

internal mitochondrial compartment, and the intermembrane space; the latter being positively charged and enclosed by the mitochondrial outer membrane (mtOM). The mtIM contains the non-bilayer phospholipid cardiolipin, which is not present in any other eukaryotic cellular membrane. Cardiolipin promotes the formation of respiratory supercomplexes, which are supramolecular assemblies based upon specific, though dynamic, interactions between individual respiratory complexes (Greggio *et al.* 2017; Lenaz *et al.* 2017). Membrane fluidity exters an influence on functional properties of proteins incorporated in the membranes (Waczulikova *et al.* 2007).

Mitochondria are the structural and functional elements of cell respiration. Cell respiration is the consumption of oxygen by electron transfer coupled to electrochemical proton translocation across the mtIM. In the process of oxidative phosphorylation (OXPHOS), the reduction of O_2 is electrochemically coupled to the transformation of energy in the form of adenosine triphosphate (ATP; Mitchell 1961, 2011). Mitochondria are the powerhouses of the cell which contain the machinery of the OXPHOS-pathways, including transmembrane respiratory complexes—proton pumps with FMN, Fe-S and cytochrome *b*, *c*, aa_3 redox systems); alternative dehydrogenases and oxidases; the coenzyme ubiquinone (Q); F-ATPase or ATP synthase; the enzymes of the tricarboxylic acid cycle and fatty acid oxidation; transporters of ions, metabolites and co-factors; and mitochondrial kinases related to energy transfer pathways. The mitochondrial proteome comprises over 1,200 proteins (Calvo *et al.* 2015; 2017), mostly encoded by nuclear DNA (nDNA), with a variety of functions, many of which are relatively well known (*e.g.,* apoptosis-regulating proteins), while others are still under investigation, or need to be identified (*e.g.,* alanine transporter).

There is a constant crosstalk between mitochondria and the other cellular components. The crosstalk between mitochondria and endoplasmic reticulum is involved in the regulation of calcium homeostasis, cell division, autophagy, differentiation, anti-viral signaling (Murley and Nunnari 2016). Cellular mitostasis is maintained through regulation at both the transcriptional and post-translational level, through cell signalling including proteostatic (*e.g.*, the ubiquitin-proteasome and autophagy-lysosome pathways), and genome stability modules throughout the cell cycle or even cell death, contributing to homeostatic regulation in response to varying energy demands and stress (Quiros *et al.* 2016). In addition to mitochondrial movement along the microtubules, mitochondrial morphology can change in response to energy requirements of the cell via processes known as fusion and fission, through which mitochondria communicate within a network, and in response to intracellular stress factors causing swelling and ultimately permeability transition.

Mitochondria typically maintain several copies of their own genome known as mitochondrial DNA (mtDNA; hundred to thousands per cell; Cummins 1998), which is maternally inherited. One exception to strictly maternal inheritance in animals is found in bivalves (Breton *et al.* 2007; White *et al.* 2008). mtDNA is 16.5 kB in length, contains 13 protein-coding genes for subunits of the transmembrane respiratory Complexes CI, CIII, CIV and F-ATPase, and also encodes 22 tRNAs and the mitochondrial 16S and 12S rRNA. Additional gene content is encoded in the mitochondrial genome, *e.g.,* microRNAs, piRNA, smithRNAs, repeat associated RNA, and even additional proteins (Duarte *et al.* 2014; Lee *et al.* 2015; Cobb *et al.* 2016). The mitochondrial genome is regulated and supplemented by nuclear-encoded mitochondrial targeted proteins.

Abbreviation: mt, as generally used in mtDNA. Mitochondrion is singular and mitochondria is plural.

'For the physiologist, mitochondria afforded the first opportunity for an experimental approach to structure-function relationships, in particular those involved in active transport, vectorial metabolism, and metabolic control mechanisms on a subcellular level' (Ernster and Schatz 1981).

1. Introduction

Mitochondria are the powerhouses of the cell with numerous physiological, molecular, and genetic functions (**Box 1**). Every study of mitochondrial health and disease is faced with **E**volution, **A**ge, **G**ender and sex, **L**ifestyle, and **E**nvironment (EAGLE) as essential background conditions intrinsic to the individual patient or subject, cohort, species, tissue and to some extent even cell line. As a large and coordinated group of laboratories and researchers, the mission of the global MitoEAGLE Network is to generate the necessary scale, type, and quality of consistent data sets and conditions to address this intrinsic complexity. Harmonization of experimental protocols and implementation of a quality control and data management system are required to interrelate results gathered across a spectrum of studies and to generate a rigorously monitored database focused on mitochondrial respiratory function. In this way, researchers within the same and across different disciplines will be positioned to compare findings across traditions and generations to an agreed upon set of clearly defined and accepted international standards.

Reliability and comparability of quantitative results depend on the accuracy of measurements under strictly-defined conditions. A conceptual framework is required to warrant meaningful interpretation and comparability of experimental outcomes carried out by research groups at different institutes. With an emphasis on quality of research, collected data can be useful far beyond the specific question of a particular experiment. Enabling meta-analytic studies is the most economic way of providing robust answers to biological questions (Cooper *et al.* 2009). Vague or ambiguous jargon can lead to confusion and may relegate valuable signals to wasteful noise. For this reason, measured values must be expressed in standard units for each parameter used to define mitochondrial respiratory function. Harmonization of nomenclature and definition of technical terms are essential to improve the awareness of the intricate meaning of current and past scientific vocabulary, for documentation and integration into databases in general, and quantitative modelling in particular (Beard 2005). The focus on coupling states and fluxes through metabolic pathways of aerobic energy transformation in mitochondrial preparations is a first step in the attempt to generate a conceptually-oriented nomenclature in bioenergetics and mitochondrial physiology. Coupling states of intact cells, the protonmotive force, and respiratory control by fuel substrates and specific inhibitors of respiratory enzymes will be reviewed in subsequent communications.

2. Oxidative phosphorylation and coupling states in mitochondrial preparations

'*Every professional group develops its own technical jargon for talking about matters of critical concern ... People who know a word can share that idea with other members of their group, and a shared vocabulary is part of the glue that holds people together and allows them to create a shared culture*' (Miller 1991).

Mitochondrial preparations are defined as either isolated mitochondria, or tissue and cellular preparations in which the barrier function of the plasma membrane is disrupted. Since this entails the loss of cell viability, mitochondrial preparations are not studied *in vivo*. In contrast to isolated mitochondria and tissue homogenate preparations, mitochondria in permeabilized tissues and cells are *in situ* relative to the plasma membrane. The plasma membrane separates the intracellular compartment including the cytosol, nucleus, and organelles from the environment of the cell. The plasma membrane consists of a lipid bilayer, embedded proteins, and attached organic molecules that collectively control the selective permeability of ions, organic molecules, and particles across the cell boundary. The intact plasma membrane prevents the passage of many water-soluble mitochondrial substrates and inorganic ions—such as succinate, adenosine diphosphate (ADP) and inorganic phosphate (P_i),

that must be controlled at kinetically-saturating concentrations for the analysis of respiratory capacities; this limits the scope of investigations into mitochondrial respiratory function in intact cells.

The cholesterol content of the plasma membrane is high compared to mitochondrial membranes. Therefore, mild detergents—such as digitonin and saponin—can be applied to selectively permeabilize the plasma membrane by interaction with cholesterol and allow free exchange of organic molecules and inorganic ions between the cytosol and the immediate cell environment, while maintaining the integrity and localization of organelles, cytoskeleton, and the nucleus. Application of optimum concentrations of permeabilization agents (mild detergents or toxins) leads to the complete loss of cell viability, tested by nuclear staining and washout of cytosolic marker enzymes—such as lactate dehydrogenase, while mitochondrial function remains intact. The respiration rate of isolated mitochondria remains unaltered after the addition of low concertations of digitonin or saponin. In addition to mechanical permeabilization during homogenization of tissue, peremeabilization agents may be applied to ensure permeabilization of all cells. Suspensions of cells permeabilized in the respiration chamber and crude tissue homogenates contain all components of the cell at highly dilute concentrations. All mitochondria are retained in chemically-permeabilized mitochondrial preparations and crude tissue homogenates. In the preparation of isolated mitochondria, the cells or tissues are homogenized, and the mitochondria are separated from other cell fractions and purified by differential centrifugation, entailing the loss of a fraction of mitochondria. Typical mitochondrial recovery ranges from 30% to 80%. Maximization of the purity of isolated mitochondria may compromise not only the mitochondrial yield but also the structural and functional integrity. Therefore, protocols to isolate mitochondria need to be optimized according to each study. The term mitochondrial preparation does not include further fractionation of mitochondrial components, neither submitochondrial particles.
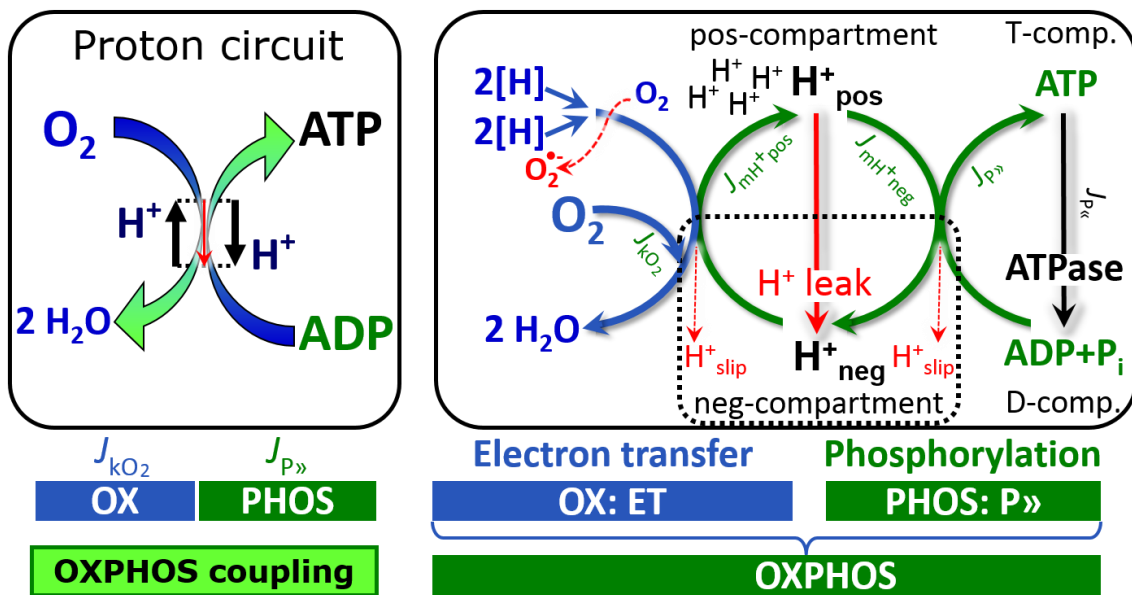
2.1. Respiratory control and coupling

Respiratory coupling control states are established in studies of mitochondrial preparations to obtain reference values for various output variables. Physiological conditions *in vivo* deviate from these experimentally obtained states. Since kinetically-saturating concentrations, *e.g.,* of ADP or oxygen, may not apply to physiological intracellular conditions, relevant information is obtained in studies of kinetic responses to variations in [ADP] or [O_2] in the range between kinetically-saturating concentrations and anoxia (Gnaiger 2001).

The steady-state: Mitochondria represent a thermodynamically open system in non-equilibrium states of biochemical energy transformation. State variables (protonmotive force; redox states) and metabolic *rates* (fluxes) are measured in defined mitochondrial respiratory *states*. Steady-states can be obtained only in open systems, in which changes by *internal* transformations, *e.g.*, O_2 consumption, are instantaneously compensated for by *external* fluxes, *e.g.*, O_2 supply, preventing a change of oxygen concentration in the system (Gnaiger 1993b). Mitochondrial respiratory states monitored in closed systems satisfy the criteria of pseudo-steady states for limited periods of time, when changes in the system (concentrations of O_2, fuel substrates, ADP, P_i, H^+) do not exert significant effects on metabolic fluxes (respiration, phosphorylation). Such pseudo-steady states require respiratory media with sufficient buffering capacity and substrates maintained at kinetically-saturating concentrations, and thus depend on the kinetics of the processes under investigation.

Specification of biochemical dose: Substrates, uncouplers, inhibitors, and other biochemical reagents are titrated to dissect mitochondrial function. Nominal concentrations of these substances are usually reported as initial amount of substance concentration [$mol \cdot L^{-1}$] in the incubation medium. When aiming at the measurement of kinetically saturated processes—such as OXPHOS-capacities, the concentrations for substrates can be chosen according to the

apparent equilibrium constant, K_m'. In the case of hyperbolic kinetics, only 80% of maximum respiratory capacity is obtained at a substrate concentration of four times the K_m', whereas substrate concentrations of 5, 9, 19 and 49 times the K_m' are theoretically required for reaching 83%, 90%, 95% or 98% of the maximal rate (Gnaiger 2001). Other reagents are chosen to inhibit or alter some process. The amount of these chemicals in an experimental incubation is selected to maximize effect, yet not lead to unacceptable off-target consequences that would adversely affect the data being sought. Specifying the amount of substance in an incubation as nominal concentration in the aqueous incubation medium can be ambiguous (Doskey *et al.* 2015), particularly when lipophilic substances (oligomycin; uncouplers, permeabilization agents) or cations (TPP$^+$; fluorescent dyes such as safranin, TMRM) are applied which accumulate in biological membranes or the mitochondrial matrix. For example, a dose of digitonin of 8 fmol·cell^{-1} (10 pg·cell^{-1}; 10 µg·10^{-6} cells) is optimal for permeabilization of endothelial cells, and the concentration in the incubation medium has to be adjusted according to the cell density applied (Doerrier *et al.* 2018). Generally, dose/exposure can be specified per unit of biological sample, *i.e.*, (nominal moles of xenobiotic)/(number of cells) [mol·cell^{-1}] or, as appropriate, per mass of biological sample [mol·kg^{-1}]. This approach to specification of dose/exposure provides a scalable parameter that can be used to design experiments, help interpret a wide variety of experimental results, and provide absolute information that allows researchers worldwide to make the most use of published data (Doskey *et al.* 2015).

Fig. 2. The proton circuit and coupling in oxidative phosphorylation (OXPHOS). 2[H] indicates the reduced hydrogen equivalents of fuel substrates of the catabolic reaction k with oxygen. Oxygen flux, J_{kO_2}, through the catabolic ET-pathway, is coupled to flux through the phosphorylation-pathway of ADP to ATP, $J_{P»}$. The proton pumps of the ET-pathway drive proton flux into the positive (pos) compartment, J_{mH+pos}, generating the output protonmotive force (motive, subscript m). F-ATPase is coupled to inward proton current into the negative (neg) compartment, J_{mH+neg}, to phosphorylate ADP+P$_i$ to ATP. The system defined by the boundaries (full black line) is not a black box, but is analysed as a compartmental system. The negative compartment (neg–compartment, enclosed by the dotted line) is the matrix space, separated by the mtIM from the positive compartment (pos–compartment). ADP+P$_i$ and ATP are the substrate- and product–compartments (scalar ADP and ATP compartments, D–comp. and T–comp.), respectively. At steady-state proton turnover, $J_{∞H+}$, and ATP turnover, $J_{∞P}$, maintain concentrations constant, when $J_{mH+∞} = J_{mH+pos} = J_{mH+neg}$, and $J_{P∞} = J_{P»} = J_{P«}$. Modified from Gnaiger (2014).

419   **Phosphorylation, P», and P»/O₂ ratio:** *Phosphorylation* in the context of OXPHOS is
420   defined as phosphorylation of ADP by P_i to ATP. On the other hand, the term phosphorylation
421   is used generally in many contexts, *e.g.,* protein phosphorylation. This justifies consideration
422   of a symbol more discriminating and specific than P as used in the P/O ratio (phosphate to
423   atomic oxygen ratio), where P indicates phosphorylation of ADP to ATP or GDP to GTP. We
424   propose the symbol P» for the endergonic (uphill) direction of phosphorylation ADP→ATP,
425   and likewise the symbol P« for the corresponding exergonic (downhill) hydrolysis ATP→ADP
426   (**Fig. 2**). P» refers mainly to electrontransfer phosphorylation but may also involve substrate-
427   level phosphorylation as part of the tricarboxylic acid (TCA) cycle (succinyl-CoA ligase) and
428   phosphorylation   of   ADP   catalyzed   by   phosphoenolpyruvate   carboxykinase.
429   Transphosphorylation is performed by adenylate kinase, creatine kinase, hexokinase and
430   nucleoside diphosphate kinase. In isolated mammalian mitochondria, ATP production
431   catalyzed by adenylate kinase (2 ADP ↔ ATP + AMP) proceeds without fuel substrates in the
432   presence of ADP (Komlódi and Tretter 2017). Kinase cycles are involved in intracellular energy
433   transfer and signal transduction for regulation of energy flux.
434   The P»/O₂ ratio (P»/4 e⁻) is two times the 'P/O' ratio (P»/2 e⁻) of classical bioenergetics.
435   P»/O₂ is a generalized symbol, independent phosphorylation assessment by determination of P_i
436   consumption (P_i/O₂ flux ratio), ADP depletion (ADP/O₂ flux ratio), or ATP production
437   (ATP/O₂ flux ratio). The mechanistic P»/O₂ ratio—or P»/O₂ stoichiometry—is calculated from
438   the proton–to–oxygen and proton–to–phosphorylation coupling stoichiometries (**Fig. 1A**),

439

440
$$P»/O_2 \; = \; \frac{H^+_{pos}/O_2}{H^+_{neg}/P»} \tag{1}$$

441

442   The H^+_{pos}/O₂ *coupling stoichiometry* (referring to the full 4 electron reduction of O₂) depends
443   on the ET-pathway control state which defines the relative involvement of the three coupling
444   sites (CI, CIII and CIV) in the catabolic pathway of electrons to O₂. This varies with: (*1*) a
445   bypass of CI by single or multiple electron input into the Q-junction; and (*2*) a bypass of CIV
446   by involvement of AOX. H^+_{pos}/O₂ is 12 in the ET-pathways involving CIII and CIV as proton
447   pumps, increasing to 20 for the NADH-pathway (**Fig. 1A**), but a general consensus on H^+_{pos}/O₂
448   stoichiometries remains to be reached (Hinkle 2005; Wikström and Hummer 2012; Sazanov
449   2015). The H^+_{neg}/P» coupling stoichiometry (3.7; **Fig. 1A**) is the sum of 2.7 H^+_{neg} required by
450   the F-ATPase of vertebrate and most invertebrate species (Watt *et al.* 2010) and the proton
451   balance in the translocation of ADP, ATP and P_i (**Fig. 1B**). Taken together, the mechanistic
452   P»/O₂ ratio is calculated at 5.4 and 3.3 for NADH- and succinate-linked respiration, respectively
453   (Eq. 1). The corresponding classical P»/O ratios (referring to the 2 electron reduction of 0.5 O₂)
454   are 2.7 and 1.6 (Watt *et al.* 2010), in agreement with the measured P»/O ratio for succinate of
455   1.58 ± 0.02 (Gnaiger *et al.* 2000).
456   The effective P»/O₂ flux ratio ($Y_{P»/O_2} = J_{P»}/J_{kO_2}$) is diminished relative to the mechanistic
457   P»/O₂ ratio by intrinsic and extrinsic uncoupling and dyscoupling (**Fig. 3**). Such generalized
458   uncoupling is different from switching to mitochondrial pathways that involve fewer than three
459   proton pumps ('coupling sites': Complexes CI, CIII and CIV), bypassing CI through multiple
460   electron entries into the Q-junction, or CIII and CIV through AOX (**Fig. 1**). Reprogramming of
461   mitochondrial pathways may be considered as a switch of gears (changing the stoichiometry)
462   rather than uncoupling (loosening the stoichiometry). In addition, $Y_{P»/O_2}$ depends on several
463   experimental conditions of flux control, increasing as a hyperbolic function of [ADP] to a
464   maximum value (Gnaiger 2001).
465   **Control and regulation:** The terms metabolic *control* and *regulation* are frequently used
466   synonymously, but are distinguished in metabolic control analysis: 'We could understand the
467   regulation as the mechanism that occurs when a system maintains some variable constant over
468   time, in spite of fluctuations in external conditions (homeostasis of the internal state). On the

other hand, metabolic control is the power to change the state of the metabolism in response to an external signal' (Fell 1997). Respiratory control may be induced by experimental control signals that *exert* an influence on: (*1*) ATP demand and ADP phosphorylation-rate; (*2*) fuel substrate composition, pathway competition; (*3*) available amounts of substrates and oxygen, *e.g.*, starvation and hypoxia; (*4*) the protonmotive force, redox states, flux–force relationships, coupling and efficiency; (*5*) Ca^{2+} and other ions including H^+; (*6*) inhibitors, *e.g.*, nitric oxide or intermediary metabolites such as oxaloacetate; (*7*) signalling pathways and regulatory proteins, *e.g.,* insulin resistance, transcription factor hypoxia inducible factor 1. *Mechanisms* of respiratory control and regulation include adjustments of: (*1*) enzyme activities by allosteric mechanisms and phosphorylation; (*2*) enzyme content, concentrations of cofactors and conserved moieties—such as adenylates, nicotinamide adenine dinucleotide [$NAD^+/NADH$], coenzyme Q, cytochrome *c*); (*3*) metabolic channeling by supercomplexes; and *(4)* mitochondrial density (enzyme concentrations and membrane area) and morphology (cristae folding, fission and fusion). Mitochondria are targeted directly by hormones, thereby affecting their energy metabolism (Lee *et al.* 2013; Gerö and Szabo 2016; Price and Dai 2016; Moreno *et al.* 2017). Evolutionary or acquired differences in the genetic and epigenetic basis of mitochondrial function (or dysfunction) between subjects and gene therapy; age; gender, biological sex, and hormone concentrations; life style including exercise and nutrition; and environmental issues including thermal, atmospheric, toxicological and pharmacological factors, exert an influence on all control mechanisms listed above. For reviews, see Brown 1992; Gnaiger 1993a, 2009; 2014; Paradies *et al.* 2014; Morrow *et al.* 2017.

Respiratory control and response: Lack of control by a metabolic pathway, *e.g.,* phosphorylation-pathway, means that there will be no response to a variable activating it, *e.g.,* [ADP]. The reverse, however, is not true as the absence of a response to [ADP] does not exclude the phosphorylation-pathway from having some degree of control. The degree of control of a component of the OXPHOS-pathway on an output variable—such as oxygen flux, will in general be different from the degree of control on other outputs—such as phosphorylation-flux or proton leak flux. Therefore, it is necessary to be specific as to which input and output are under consideration (Fell 1997).

Respiratory coupling control and ET-pathway control: Respiratory control refers to the ability of mitochondria to adjust oxygen consumption in response to external control signals by engaging various mechanisms of control and regulation. Respiratory control is monitored in a mitochondrial preparation under conditions defined as respiratory states. When phosphorylation of ADP to ATP is stimulated or depressed, an increase or decrease is observed in electron flux linked to oxygen consumption in respiratory coupling states of intact mitochondria ('controlled states' in the classical terminology of bioenergetics). Alternatively, coupling of electron transfer with phosphorylation is disengaged by disruption of the integrity of the mtIM or by uncouplers, functioning like a clutch in a mechanical system. The corresponding coupling control state is characterized by high levels of oxygen consumption without control by P» ('uncontrolled state').

ET-pathway control states are obtained in mitochondrial preparations by depletion of endogenous substrates and addition to the mitochondrial respiration medium of fuel substrates (CHNO; 2[H] in **Fig. 2**) and specific inhibitors, activating selected mitochondrial catabolic pathways, k (**Fig. 1**). Coupling control states and pathway control states are complementary, since mitochondrial preparations depend on an exogenous supply of pathway-specific fuel substrates and oxygen (Gnaiger 2014).

Coupling: In mitochondrial electron transfer (**Fig. 1**), vectorial transmembrane proton flux is coupled through the proton pumps CI, CIII and CIV to the catabolic flux of scalar reactions, collectively measured as oxygen flux (**Fig. 2**). Thus mitochondria are elements of energy transformation. Energy cannot be lost or produced in any internal process (First Law of thermodynamics). Open and closed systems can gain or loose energy only by external fluxes—

520 by exchange with the environment. Energy is a conserved quantity. Therefore, energy can
521 neither be produced by mitochondria, nor is there any internal process without energy
522 conservation. Exergy is defined as the 'free energy' with the potential to perform work.
523 *Coupling* is the mechanistic linkage of an exergonic process (spontaneous, negative exergy
524 change) with an endergonic process (positive exergy change) in energy transformations which
525 conserve part of the exergy that would be irreversible lost or dissipated in an uncoupled process.
526   **Uncoupling:** Uncoupling of mitochondrial respiration is a general term comprising
527 diverse mechanisms. Differences of terms—uncoupled *vs.* noncoupled—are easily overlooked,
528 although they relate to different mechanisms of uncoupling (**Fig. 3**).
529   1. Proton leak across the mtIM from the pos– to the neg–compartment (**Fig. 2**);
530   2. Cycling of other cations, strongly stimulated by permeability transition;
531   3. Proton slip in the proton pumps when protons are effectively not pumped (CI, CIII and
532   CIV) or are not driving phosphorylation (F-ATPase);
533   4. Loss of compartmental integrity when electron transfer is acoupled;
534   5. Electron leak in the loosely coupled univalent reduction of oxygen (O_2; dioxygen) to
535   superoxide ($O_2^{\bullet-}$; superoxide anion radical).
536
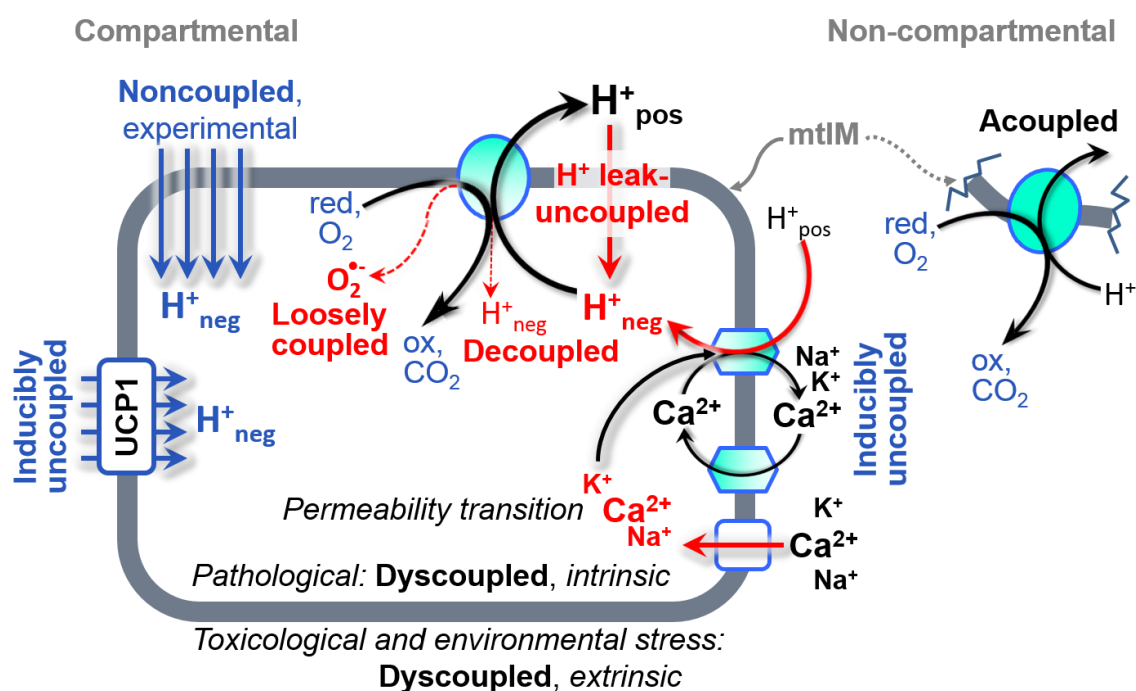
538 **Fig 3. Mechanisms of respiratory uncoupling.** An intact mitochondrial inner membrane,
539 mtIM, is required for vectorial, compartmental coupling. 'Acoupled' respiration is the
540 consequence of structural disruption with catalytic activity of non-compartmental
541 mitochondrial fragments. Inducibly uncoupled (activation of UCP1) and experimentally
542 noncoupled respiration (titration of protonophores) stimulate respiration to maximum oxygen
543 flux. H^+ leak-uncoupled, decoupled, and loosely coupled respiration are components of intrinsic
544 uncoupling. Pathological dysfunction may affect all types of uncoupling, including
545 permeability transition, causing intrinsically dyscoupled respiration. Similarly, toxicological
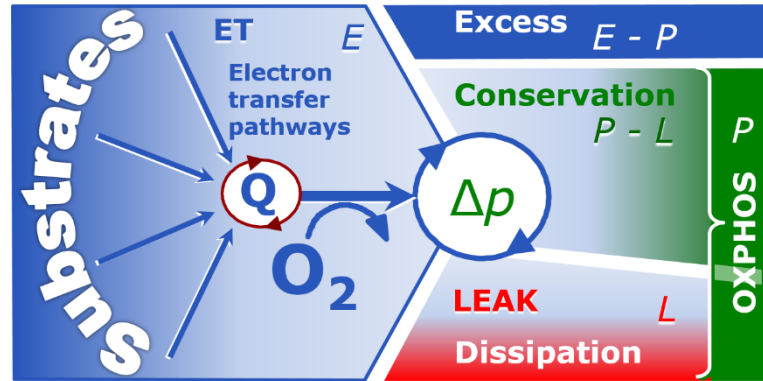546 and environmental stress factors can cause extrinsically dyscoupled respiration.
547

548 *2.2. Coupling states and respiratory rates*
549

550   **Respiratory capacities in coupling control states:** To extend the classical nomenclature
551 on mitochondrial coupling states (Section 2.3) by a concept-driven terminology that
552 incorporates explicitly information on the nature of respiratory states, the terminology must be

general and not restricted to any particular experimental protocol or mitochondrial preparation (Gnaiger 2009). We focus primarily on the conceptual 'why', along with clarification of the experimental 'how'. Respiratory capacities delineate, comparable to channel capacity in information theory (Schneider 2006), the upper bound of the rate of respiration measured in defined coupling control states and electron transfer-pathway (ET-pathway) states (**Fig. 4**).

Fig. 4. Four-compartment model of oxidative phosphorylation. Respiratory states (ET, OXPHOS, LEAK; **Table 1**) and corresponding rates (E, P, L) are connected by the protonmotive force, Δp. ET-capacity, E, is partitioned into (*1*) dissipative LEAK-respiration, L, when the Gibbs energy change of catabolic O_2 consumption is irreversibly lost, (*2*) net OXPHOS-capacity, $P-L$, with partial conservation of the capacity to perform work, and (*3*) the excess capacity, $E-P$. Modified from Gnaiger (2014).

Table 1. Coupling states and residual oxygen consumption in mitochondrial preparations in relation to respiration- and phosphorylation-rate, J_{kO_2} and $J_{P»}$, and protonmotive force, Δp. Coupling states are established at kinetically-saturating concentrations of fuel substrates and O_2.

State	J_{kO_2}	$J_{P»}$	Δp	Inducing factors	Limiting factors
LEAK	L; low, cation leak-dependent respiration	0	max.	proton leak, slip, and cation cycling	$J_{P»} = 0$: (*1*) without ADP, L_N; (*2*) max. ATP/ADP ratio, L_T; or (*3*) inhibition of the phosphorylation-pathway, L_{Omy}
OXPHOS	P; high, ADP-stimulated respiration	max.	high	kinetically-saturating [ADP] and [P_i]	$J_{P»}$ by phosphorylation-pathway; or J_{kO_2} by ET-capacity
ET	E; max., noncoupled respiration	0	low	optimal external uncoupler concentration for max. $J_{O_2,E}$	J_{kO_2} by ET-capacity
ROX	Rox; min., residual O_2 consumption	0	0	$J_{O_2,Rox}$ in non-ET-pathway oxidation reactions	full inhibition of ET-pathway; or absence of fuel substrates

To provide a diagnostic reference for respiratory capacities of core energy metabolism, the capacity of *oxidative phosphorylation*, OXPHOS, is measured at kinetically-saturating concentrations of ADP and P_i. The *oxidative* ET-capacity reveals the limitation of OXPHOS-capacity mediated by the *phosphorylation*-pathway. The ET- and phosphorylation-pathways comprise coupled segments of the OXPHOS-system. ET-capacity is measured as noncoupled respiration by application of *external uncouplers*. The contribution of *intrinsically uncoupled*

584 oxygen consumption is studied in the absence of ADP—by not stimulating phosphorylation, or
585 by inhibition of the phosphorylation-pathway. The corresponding states are collectively
586 classified as LEAK-states, when oxygen consumption compensates mainly for ion leaks,
587 including the proton leak. Defined coupling states are induced by: (*1*) adding cation chelators
588 such as EGTA, binding free Ca^{2+} and thus limiting cation cycling; (*2*) adding ADP and P_i; (*3*)
589 inhibiting the phosphorylation-pathway; and (*4*) uncoupler titrations, while maintaining a
590 defined ET-pathway state with constant fuel substrates and inhibitors of specific branches of
591 the ET-pathway (**Fig. 1**).

592   The three coupling states, ET, LEAK and OXPHOS, are shown schematically with the
593 corresponding respiratory rates, abbreviated as *E*, *L* and *P*, respectively (**Fig. 4**). We distinguish
594 metabolic *pathways* from metabolic *states* and the corresponding metabolic *rates*; for example:
595 ET-pathways (**Fig. 4**), ET-state (**Fig. 5C**), and ET-capacity, *E*, respectively (**Table 1**). The
596 protonmotive force is *high* in the OXPHOS-state when it drives phosphorylation, *maximum* in
597 the LEAK-state of coupled mitochondria, driven by LEAK-respiration at a minimum back flux
598 of cations to the matrix side, and *very low* in the ET-state when uncouplers short-circuit the
599 proton cycle (**Table 1**).

600   *E* may exceed or be equal to *P*. *E* > *P* is observed in many types of mitochondria, varying
601 between species, tissues and cell types (Gnaiger 2009). *E-P* is the excess ET-capacity pushing
602 the phosphorylation-flux (**Fig. 1B**) to the limit of its *capacity of utilizing* the protonmotive force.
603 In addition, the magnitude of *E-P* depends on the tightness of respiratory coupling or degree of
604 uncoupling, since an increase of *L* causes *P* to increase towards the limit of *E*. The *excess E-P*
605 capacity, *E-P*, therefore, provides a sensitive diagnostic indicator of specific injuries of the
606 phosphorylation-pathway, under conditions when *E* remains constant but *P* declines relative to
607 controls (**Fig. 4**). Substrate cocktails supporting simultaneous convergent electron transfer to
608 the Q-junction for reconstitution of TCA cycle function establish pathway control states with
609 high ET-capacity, and consequently increase the sensitivity of the *E-P* assay.

610   *E* cannot theoretically be lower than *P*. *E* < *P* must be discounted as an artefact, which
611 may be caused experimentally by: (*1*) loss of oxidative capacity during the time course of the
612 respirometric assay, since *E* is measured subsequently to *P*; (*2*) using insuffient uncoupler
613 concentrations; (*3*) using high uncoupler concentrations which inhibit ET (Gnaiger 2008); (*4*)
614 high oligomycin concentrations applied for measurement of *L* before titrations of uncoupler,
615 when oligomycin exerts an inhibitory effect on *E*. On the other hand, the excess ET-capacity is
616 overestimated if non-saturating [ADP] or [P_i] are used. See State 3 in the next section.

617   The net OXPHOS-capacity is calculated by subtracting *L* from *P* (**Fig. 4**). Then the net
618 P»/O_2 equals P»/(*P-L*), wherein the dissipative LEAK component in the OXPHOS-state may
619 be overestimated. This can be avoided by measuring LEAK-respiration in a state when the
620 protonmotive force is adjusted to its slightly lower value in the OXPHOS-state—by titration of
621 an ET inhibitor (Divakaruni and Brand 2011). Any turnover-dependent components of proton
622 leak and slip, however, are underestimated under these conditions (Garlid *et al.* 1993). In
623 general, it is inappropriate to use the term *ATP production* or *ATP turnover* for the difference
624 of oxygen consumption measured in states *P* and *L*. The difference *P-L* is the upper limit of the
625 part of OXPHOS-capacity that is freely available for ATP production (corrected for LEAK-
626 respiration) and is fully coupled to phosphorylation with a maximum mechanistic stoichiometry
627 (**Fig. 4**).

628   **LEAK-state** (**Fig. 5A**): The LEAK-state is defined as a state of mitochondrial respiration
629 when O_2 flux mainly compensates for ion leaks in the absence of ATP synthesis, at kinetically-
630 saturating concentrations of O_2 and respiratory fuel substrates. LEAK-respiration is measured
631 to obtain an estimate of *intrinsic uncoupling* without addition of an experimental uncoupler: (*1*)
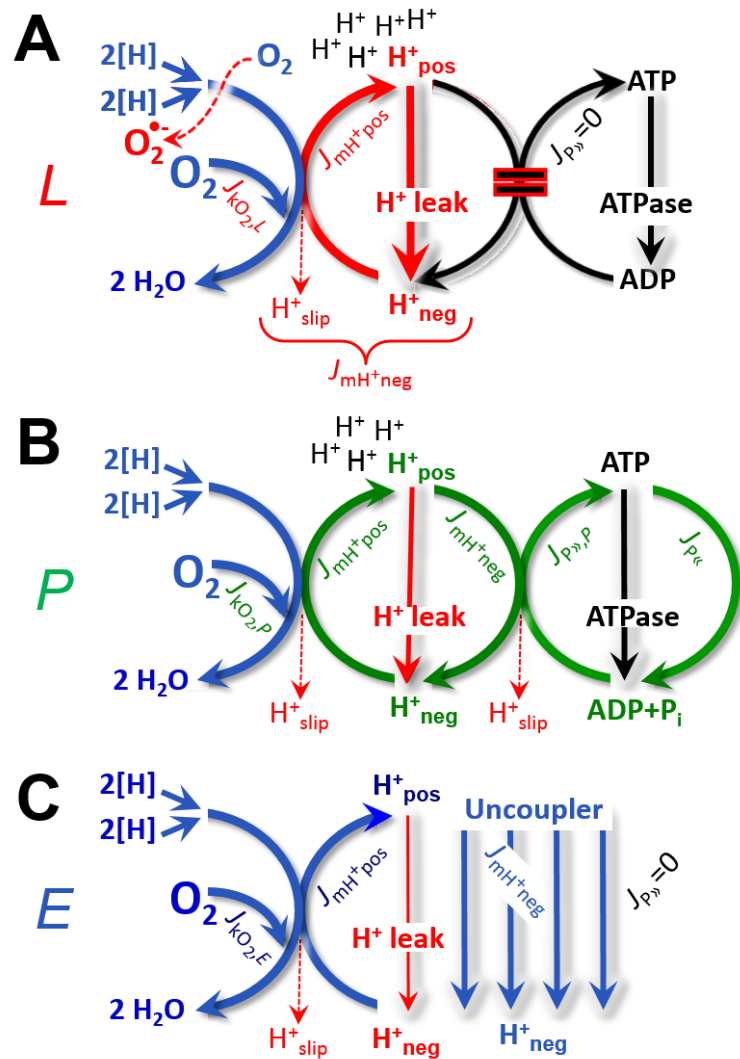
in the absence of adenylates; (2) after depletion of ADP at a maximum ATP/ADP ratio; or (3) after inhibition of the phosphorylation-pathway by inhibitors of F-ATPase—such as oligomycin, or of adenine nucleotide translocase—such as carboxyatractyloside.

Adjustment of the nominal concentration of these inhibitors to the density of biological sample applied can minimize or avoid inhibitory side-effects exerted on ET-capacity or even some dyscoupling.

Proton leak and uncoupled respiration: Proton leak is a leak current of protons. The intrinsic proton leak is the *uncoupled* process in which protons diffuse across the mtIM in the dissipative direction of the downhill protonmotive force without coupling to phosphorylation (**Fig. 5A**). The proton leak flux depends non-linearly on the protonmotive force (Garlid *et al.* 1989; Divakaruni and Brand 2011), it is a property of the mtIM and may be enhanced due to possible contaminations by free fatty acids. Inducible uncoupling mediated by uncoupling protein 1 (UCP1) is physiologically controlled, *e.g.*, in brown adipose tissue. UCP1 is a member of the mitochondrial carrier family which is involved in the translocation of protons across the mtIM (Klingenberg 2017). Consequently, the short-circuit diminishes the protonmotive force and stimulates electron transfer to O_2 and heat dissipation without phosphorylation of ADP.

Fig. 5. Respiratory coupling states. A: LEAK-state and rate, L: Phosphorylation is arrested, $J_{P»} = 0$, and catabolic oxygen flux, $J_{kO_2,L}$, is controlled mainly by the proton leak, $J_{mH^+neg,L}$, at maximum protonmotive force (**Fig. 3**). **B: OXPHOS-state and rate, P:** Phosphorylation, $J_{P»}$, is stimulated by kinetically-saturating [ADP] and [P_i], and is supported by a high protonmotive force. O_2 flux, $J_{kO_2,P}$, is well-coupled at a P»/O_2 ratio of $J_{P»,P}/J_{O_2,P}$. **C: ET-state and rate, E:** Noncoupled respiration, $J_{kO2,E}$, is maximum at optimum exogenous uncoupler concentration and phosphorylation is zero, $J_{P»} = 0$. See also **Fig. 2**.

Cation cycling: There can be other cation contributors to leak current including calcium and probably magnesium. Calcium current is balanced by mitochondrial Na^+/Ca^{2+} exchange, which is balanced by Na^+/H^+ or K^+/H^+ exchanges. This is another effective uncoupling mechanism different from proton leak.

Table 2. Terms on respiratory coupling and uncoupling.

Term	J_{kO_2}	P»/O$_2$	Note
acoupled		0	electron transfer in mitochondrial fragments without vectorial proton translocation (**Fig. 3**)
uncoupled	L	0	non-phosphorylating LEAK-respiration (**Fig. 5A**)
proton leak-uncoupled		0	component of L, H$^+$ diffusion across the mtIM (**Fig. 3**)
decoupled		0	component of L, proton slip (**Fig. 3**)
loosely coupled		0	component of L, lower coupling due to superoxide formation and bypass of proton pumps (**Fig. 3**)
dyscoupled		0	pathologically, toxicologically, environmentally increased uncoupling, mitochondrial dysfunction
inducibly uncoupled		0	by UCP1 or cation (*e.g.,* Ca^{2+}) cycling (**Fig. 3**)
noncoupled	E	0	non-phosphorylating respiration stimulated to maximum flux at optimum exogenous uncoupler concentration (**Fig. 5C**)
well-coupled	P	high	phosphorylating respiration with an intrinsic LEAK component (**Fig. 5B**)
fully coupled	$P - L$	max.	OXPHOS-capacity corrected for LEAK-respiration (**Fig. 4**)

(Bracket spanning uncoupled through inducibly uncoupled rows, labeled: intrinsic, no protonophore added)

Proton slip and decoupled respiration: Proton slip is the *decoupled* process in which protons are only partially translocated by a proton pump of the ET-pathways and slip back to the original compartment. The proton leak is the dominant contributor to the overall leak current in mammalian mitochondria incubated under physiological conditions at 37 °C, whereas proton slip is increased at lower experimental temperature (Canton *et al.* 1995). Proton slip can also happen in association with the F-ATPase, in which the proton slips downhill across the pump to the matrix without contributing to ATP synthesis. In each case, proton slip is a property of the proton pump and increases with the pump turnover rate.

Electron leak and loosely coupled respiration: Superoxide production by the ETS leads to a bypass of proton pumps and correspondingly lower P»/O$_2$ ratio. This depends on the actual site of electron leak and the scavenging of hydrogen peroxide by cytochrome *c*, whereby electrons may re-enter the ETS with proton translocation by CIV.

Loss of compartmental integrity and acoupled respiration: Electron transfer and O$_2$ consumption proceed without compartmental proton translocation in disrupted mitochondrial fragments. Such fragments form during mitochondrial isolation, and may not fully fuse to re-establish structurally intact mitochondria. Loss of mtIM integrity, therefore, is the cause of acoupled respiration, which is a nonvectorial dissipative process without control by the protonmotive force.

Dyscoupled respiration: Mitochondrial injuries may lead to *dyscoupling* as a pathological or toxicological cause of *uncoupled* respiration. Dyscoupling may involve any type of uncoupling mechanism, *e.g.*, opening the permeability transition pore. Dyscoupled respiration is distinguished from the experimentally induced *noncoupled* respiration in the ET-state (**Fig. 3**).

OXPHOS-state (**Fig. 5B**): The OXPHOS-state is defined as the respiratory state with kinetically-saturating concentrations of O$_2$, respiratory and phosphorylation substrates, and

absence of exogenous uncoupler, which provides an estimate of the maximal respiratory capacity in the OXPHOS-state for any given ET-pathway state. Respiratory capacities at kinetically-saturating substrate concentrations provide reference values or upper limits of performance, aiming at the generation of data sets for comparative purposes. Physiological activities and effects of substrate kinetics can be evaluated relative to the OXPHOS-capacity.

As discussed previously, 0.2 mM ADP does not fully saturate flux in isolated mitochondria (Gnaiger 2001; Puchowicz *et al.* 2004); greater ADP concentration is required, particularly in permeabilized muscle fibres and cardiomyocytes, to overcome limitations by intracellular diffusion and by the reduced conductance of the mtOM (Jepihhina *et al.* 2011, Illaste *et al.* 2012, Simson *et al.* 2016), either through interaction with tubulin (Rostovtseva *et al.* 2008) or other intracellular structures (Birkedal *et al.* 2014). In permeabilized muscle fibre bundles of high respiratory capacity, the apparent K_m for ADP increases up to 0.5 mM (Saks *et al.* 1998), consistent with experimental evidence that >90% saturation is reached only at >5 mM ADP (Pesta and Gnaiger 2012). Similar ADP concentrations are also required for accurate determination of OXPHOS-capacity in human clinical cancer samples and permeabilized cells (Klepinin *et al.* 2016; Koit *et al.* 2017). Whereas 2.5 to 5 mM ADP is sufficient to obtain the actual OXPHOS-capacity in many types of permeabilized tissue and cell preparations, experimental validation is required in each specific case.

Electron transfer-state (**Fig. 5C**): The ET-state is defined as the *noncoupled* state with kinetically-saturating concentrations of O_2, respiratory substrate and optimum *exogenous* uncoupler concentration for maximum O_2 flux, as an estimate of ET-capacity. Inhibition of respiration is observed at higher than optimum uncoupler concentrations. As a consequence of the nearly collapsed protonmotive force, the driving force is insufficient for phosphorylation, and $J_{P»} = 0$.

ROX state and *Rox*: Besides the three fundamental coupling states of mitochondrial preparations, the state of residual oxygen consumption, ROX, is relevant to assess respiratory function. ROX is not a coupling state. The rate of residual oxygen consumption, *Rox*, is defined as O_2 consumption due to oxidative side reactions remaining after inhibition of ET—with rotenone, malonic acid and antimycin A. Cyanide and azide not only inhibit CIV but also several peroxidases involved in *Rox*. ROX represents a baseline that is used to correct mitochondrial respiration in defined coupling states. *Rox* is not necessarily equivalent to non-mitochondrial respiration, considering oxygen-consuming reactions in mitochondria not related to ET—such as oxygen consumption in reactions catalyzed by monoamine oxidases (type A and B), monooxygenases (cytochrome P450 monooxygenases), dioxygenase (sulfur dioxygenase and trimethyllysine dioxygenase), and several hydoxylases. Mitochondrial preparations, especially those obtained from liver, may be contaminated by peroxisomes. This fact makes the exact determination of mitochondrial oxygen consumption and mitochondria-associated generation of reactive oxygen species complicated (Schönfeld *et al.* 2009). The dependence of ROX-linked oxygen consumption needs to be studied in detail together with non-ET enzyme activities, availability of specific substrates, oxygen concentration, and electron leakage leading to the formation of reactive oxygen species.

2.3. Classical terminology for isolated mitochondria

> *'When a code is familiar enough, it ceases appearing like a code; one forgets that there is a decoding mechanism. The message is identical with its meaning'* (Hofstadter 1979).

Chance and Williams (1955; 1956) introduced five classical states of mitochondrial respiration and cytochrome redox states. **Table 3** shows a protocol with isolated mitochondria in a closed respirometric chamber, defining a sequence of respiratory states. States and rates are not specifically distinguished in this nomenclature.

Table 3. Metabolic states of mitochondria (Chance and Williams, 1956; Table V).

State	$[O_2]$	ADP level	Substrate level	Respiration rate	Rate-limiting substance
1	>0	low	low	slow	ADP
2	>0	high	~0	slow	substrate
3	>0	high	high	fast	respiratory chain
4	>0	low	high	slow	ADP
5	0	high	high	0	oxygen

State 1 is obtained after addition of isolated mitochondria to air-saturated isoosmotic/isotonic respiration medium containing P_i, but no fuel substrates and no adenylates, *i.e.*, AMP, ADP, ATP.

State 2 is induced by addition of a 'high' concentration of ADP (typically 100 to 300 µM), which stimulates respiration transiently on the basis of endogenous fuel substrates and phosphorylates only a small portion of the added ADP. State 2 is then obtained at a low respiratory activity limited by exhausted endogenous fuel substrate availability (**Table 3**). If addition of specific inhibitors of respiratory complexes—such as rotenone—does not cause a further decline of oxygen consumption, State 2 is equivalent to the state of residual oxygen consumption, ROX (See below.). If inhibition is observed, undefined endogenous fuel substrates are a confounding factor of pathway control, contributing to the effect of subsequently externally added substrates and inhibitors. In contrast to the original protocol, an alternative sequence of titration steps is frequently applied, in which the alternative 'State 2' has an entirely different meaning, when this second state is induced by addition of fuel substrate without ADP (LEAK-state; in contrast to State 2 defined in **Table 1** as a ROX state), followed by addition of ADP.

State 3 is the state stimulated by addition of fuel substrates while the ADP concentration is still high (**Table 3**) and supports coupled energy transformation through oxidative phosphorylation. 'High ADP' is a concentration of ADP specifically selected to allow the measurement of State 3 to State 4 transitions of isolated mitochondria in a closed respirometric chamber. Repeated ADP titration re-establishes State 3 at 'high ADP'. Starting at oxygen concentrations near air-saturation (ca. 200 µM O_2 at sea level and 37 °C), the total ADP concentration added must be low enough (typically 100 to 300 µM) to allow phosphorylation to ATP at a coupled rate of oxygen consumption that does not lead to oxygen depletion during the transition to State 4. In contrast, kinetically-saturating ADP concentrations usually are 10-fold higher than 'high ADP', *e.g.,* 2.5 mM in isolated mitochondria. The abbreviation State 3u is occasionally used in bioenergetics, to indicate the state of respiration after titration of an uncoupler, without sufficient emphasis on the fundamental difference between OXPHOS-capacity (*well-coupled* with an *endogenous* uncoupled component) and ET-capacity (*noncoupled*).

State 4 is a LEAK-state that is obtained only if the mitochondrial preparation is intact and well-coupled. Depletion of ADP by phosphorylation to ATP leads to a decline in the rate of oxygen consumption in the transition from State 3 to State 4. Under these conditions of State 4, a maximum protonmotive force and high ATP/ADP ratio are maintained. For calculation of P»/O_2 ratios the gradual decline of $Y_{P»/O_2}$ towards diminishing [ADP] at State 4 must be taken into account (Gnaiger 2001). State 4 respiration, L_T (**Table 1**), reflects intrinsic proton leak and intrinsic ATP hydrolysis activity. Oxygen consumption in State 4 is an overestimation of LEAK-respiration if the contaminating ATP hydrolysis activity recycles some ATP to ADP, $J_{P«}$, which stimulates respiration coupled to phosphorylation, $J_{P»} > 0$. This can be tested by inhibition of the phosphorylation-pathway using oligomycin, ensuring that $J_{P»} = 0$ (State 4o).

805 Alternatively, sequential ADP titrations re-establish State 3, followed by State 3 to State 4
806 transitions while sufficient oxygen is available. Anoxia may be reached, however, before
807 exhaustion of ADP (State 5).
808   **State 5** is the state after exhaustion of oxygen in a closed respirometric chamber.
809 Diffusion of oxygen from the surroundings into the aqueous solution may be a confounding
810 factor preventing complete anoxia (Gnaiger 2001). Chance and Williams (1955) provide an
811 alternative definition of State 5, which gives it the different meaning of ROX versus anoxia:
812 'State 5 may be obtained by antimycin A treatment or by anaerobiosis'.
813   In **Table 3**, only States 3 and 4 (and 'State 2' in the alternative protocol: addition of fuel
814 substrates without ADP; not included in the table) are coupling control states, with the
815 restriction that O_2 flux in State 3 may be limited kinetically by non-saturating ADP
816 concentrations (**Table 1**).

3. Normalization: fluxes and flows

3.1. Normalization: system or sample

823   The term *rate* is not sufficiently defined to be useful for reporting data (**Fig. 6**). The
824 inconsistency of the meanings of rate becomes fully apparent when considering Galileo
825 Galilei's famous principle, that 'bodies of different weight all fall at the same rate (have a
826 constant acceleration)' (Coopersmith 2010).

Fig. 6. Different meanings of *rate* may lead to confusion, if the normalization is not sufficiently specified. Results are frequently expressed as mass-specific *flux*, J_{mX}, per mg protein, dry or wet weight (mass). Cell volume, V_{cell}, may be used for normalization (volume-specific flux, J_{Vcell}), which must be clearly distinguished from flow per cell, I_{Ncell}, or flux, J_V, expressed for methodological reasons per volume of the measurement system. For details see **Table 4**.

844   **Flow per system, I:** In a generalization of electrical terms, flow as an extensive quantity
845 (I; per system) is distinguished from flux as a size-specific quantity (J; per system size) (**Fig.**
846 **6**). Electric current is flow, I_{el} [$A \equiv C \cdot s^{-1}$] per system (extensive quantity). When dividing this
847 extensive quantity by system size (cross-sectional area of a 'wire'), a size-specific quantity is
848 obtained, which is flux (current density), J_{el} [$A \cdot m^{-2} = C \cdot s^{-1} \cdot m^{-2}$].
849   **Extensive quantities:** An extensive quantity increases proportionally with system size.
850 The magnitude of an extensive quantity is completely additive for non-interacting
851 subsystems—such as mass or flow expressed per defined system. The magnitude of these
852 quantities depends on the extent or size of the system (Cohen *et al.* 2008).
853   **Size-specific quantities:** 'The adjective *specific* before the name of an extensive quantity
854 is often used to mean *divided by mass*' (Cohen *et al.* 2008). In this system-paradigm, mass-
855 specific flux is flow divided by mass of the *system* (the total mass of everything within the
856 measuring chamber or reactor). A mass-specific quantity is independent of the extent of non-
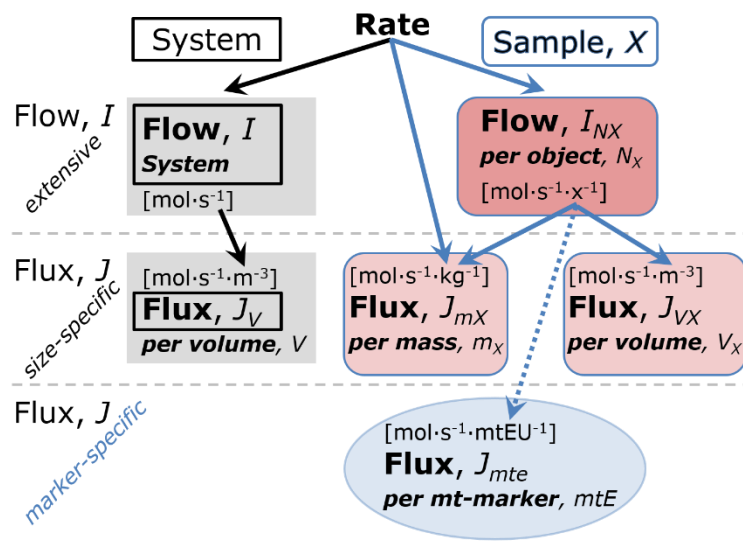
857 interacting homogenous subsystems. Tissue-specific quantities (related to the *sample* in
858 contrast to the *system*) are of fundamental interest in comparative mitochondrial physiology,
859 where *specific* refers to the *type of the sample* rather than *mass of the system*. The term *specific*,
860 therefore, must be clarified; *sample*-specific, *e.g.*, muscle mass-specific normalization, is
861 distinguished from *system*-specific quantities (mass or volume; **Fig. 6**).
862

---

863 **Box 2: Metabolic fluxes and flows: vectorial and scalar**
864
865   Fluxes are *vectors*, if they have *spatial* geometric direction in addition to magnitude.
866 Electric charge per unit time is electric flow or current, $I_{el} = dQ_{el} \cdot dt^{-1}$ [A]. When expressed per
867 unit cross-sectional area, A [m^2], a vector flux is obtained, which is current density or surface-
868 density of flow) perpendicular to the direction of flux, $J_{el} = I_{el} \cdot A^{-1}$ [A·m^{-2}] (Cohen et al. 2008).
869 For all transformations *flows*, I_{tr}, are defined as extensive quantities. Vector and scalar *fluxes*
870 are obtained as $J_{tr} = I_{tr} \cdot A^{-1}$ [mol·s^{-1}·m^{-2}] and $J_{tr} = I_{tr} \cdot V^{-1}$ [mol·s^{-1}·m^{-3}], expressing flux as an area-
871 specific vector or volume-specific vectorial or scalar quantity, respectively (Gnaiger 1993b).
872   We suggest to define: (*1*) *vectoral* fluxes, which are translocations as functions of
873 *gradients* with direction in geometric space in continuous systems; (*2*) *vectorial* fluxes, which
874 describe translocations in discontinuous systems and are restricted to information on
875 *compartmental differences* (**Fig. 2**, transmembrane proton flux); and (*3*) *scalar* fluxes, which
876 are transformations in a *homogenous* system (**Fig. 2**, catabolic O$_2$ flux, J_{kO_2}).
877   Vectorial transmembrane proton fluxes, J_{mH+pos} and J_{mH+neg}, are analyzed in a
878 heterogenous compartmental system as a quantity with *directional* but not *spatial* information.
879 Translocation of protons across the mtIM has a defined direction, either from the negative
880 compartment (matrix space; negative, neg–compartment) to the positive compartment (inter-
881 membrane space; positive, pos–compartment) or *vice versa* (**Fig. 2**). The arrows defining the
882 direction of the translocation between the two compartments may point upwards or downwards,
883 right or left, without any implication that these are actual directions in space. The pos–
884 compartment is neither above nor below the neg–compartment in a spatial sense, but can be
885 visualized arbitrarily in a figure in the upper position (**Fig. 2**). In general, the *compartmental*
886 *direction* of vectorial translocation from the neg–compartment to the pos–compartment is
887 defined by assigning the initial and final state as *ergodynamic compartments*, $H^+_{neg} \rightarrow H^+_{pos}$ or
888 $0 = -1\ H^+_{neg} + 1\ H^+_{pos}$, related to work (erg = work) that must be performed to lift the proton from
889 a lower to a higher electrochemical potential or from the lower to the higher ergodynamic
890 compartment (Gnaiger 1993b).
891   In analogy to *vectorial* translocation, the direction of a *scalar* chemical reaction, $A \rightarrow B$
892 or $0 = -1\ A + 1\ B$, is defined by assigning substrates and products, A and B, as ergodynamic
893 compartments. O$_2$ is defined as a substrate in respiratory O$_2$ consumption, which together with
894 the fuel substrates comprises the substrate compartment of the catabolic reaction (**Fig. 2**).
895 Volume-specific scalar O$_2$ flux is coupled to vectorial translocation, yielding the H^+_{pos}/O_2 ratio
896 (**Fig. 1**).
897

898
899 *3.2. Normalization for system-size: flux per chamber volume*
900
901   **System-specific flux, J_{V,O_2}:** The experimental system (experimental chamber) is part of
902 the measurement apparatus, separated from the environment as an isolated, closed, open,
903 isothermal or non-isothermal system (**Table 4**). On another level, we distinguish between (*1*)
904 the *system* with volume V and mass m defined by the system boundaries, and (*2*) the *sample* or
905 *objects* with volume V_X and mass m_X which are enclosed in the experimental chamber (**Fig. 6**).
906 Metabolic O$_2$ flow per object, $I_{O_2/X}$, increases as the mass of the object is increased. Sample
907 mass-specific O$_2$ flux, $J_{O_2/mX}$ should be independent of the mass of the sample studied in the

908 instrument chamber, but system volume-specific O_2 flux, J_{V,O_2} (per volume of the instrument
909 chamber), should increase in direct proportion to the mass of the sample in the chamber.
910 Whereas J_{V,O_2} depends on mass-concentration of the sample in the chamber, it should be
911 independent of the chamber (system) volume at constant sample mass. There are practical
912 limitations to increase the mass-concentration of the sample in the chamber, when one is
913 concerned about crowding effects and instrumental time resolution.
914   When the reactor volume does not change during the reaction, which is typical for liquid
915 phase reactions, the volume-specific *flux of a chemical reaction* r is the time derivative of the
916 advancement of the reaction per unit volume, $J_{V,rB} = d_r\xi_B/dt \cdot V^{-1}$ [$(mol \cdot s^{-1}) \cdot L^{-1}$]. The *rate of*
917 *concentration change* is dc_B/dt [$(mol \cdot L^{-1}) \cdot s^{-1}$], where concentration is $c_B = n_B/V$. There is a
918 difference between (*1*) J_{V,rO_2} [$mol \cdot s^{-1} \cdot L^{-1}$] and (*2*) rate of concentration change [$mol \cdot L^{-1} \cdot s^{-1}$].
919 These merge to a single expression only in closed systems. In open systems, external fluxes
920 (such as O_2 supply) are distinguished from internal transformations (catabolic flux, O_2
921 consumption). In a closed system, external flows of all substances are zero and O_2 consumption
922 (internal flow of catabolic reactions k), I_{kO_2} [$pmol \cdot s^{-1}$], causes a decline of the amount of O_2 in
923 the system, n_{O_2} [nmol]. Normalization of these quantities for the volume of the system, V [L ≡
924 dm^3], yields volume-specific O_2 flux, $J_{V,kO_2} = I_{kO_2}/V$ [$nmol \cdot s^{-1} \cdot L^{-1}$], and O_2 concentration, [O_2]
925 or $c_{O_2} = n_{O_2}/V$ [$\mu mol \cdot L^{-1} = \mu M = nmol \cdot mL^{-1}$]. Instrumental background O_2 flux is due to external
926 flux into a non-ideal closed respirometer; then total volume-specific flux has to be corrected for
927 instrumental background O_2 flux—O_2 diffusion into or out of the instrumental chamber. J_{V,kO_2}
928 is relevant mainly for methodological reasons and should be compared with the accuracy of
929 instrumental resolution of background-corrected flux, *e.g.*, ±1 $nmol \cdot s^{-1} \cdot L^{-1}$ (Gnaiger 2001).
930 'Metabolic' or catabolic indicates O_2 flux, J_{kO_2}, corrected for: (*1*) instrumental background O_2
931 flux; (*2*) chemical background O_2 flux due to autoxidation of chemical components added to
932 the incubation medium; and (*3*) *Rox* for O_2-consuming side reactions unrelated to the catabolic
933 pathway k.

935 *3.3. Normalization: per sample*

937   The challenges of measuring mitochondrial respiratory flux are matched by those of
938 normalization. Application of common and defined units is required for direct transfer of
939 reported results into a database. The second [s] is the *SI* unit for the base quantity *time*. It is also
940 the standard time-unit used in solution chemical kinetics. A rate may be considered as the
941 numerator and normalization as the complementary denominator, which are tightly linked in
942 reporting the measurements in a format commensurate with the requirements of a database.
943 Normalization (**Table 4**) is guided by physicochemical principles, methodological
944 considerations, and conceptual strategies (**Fig. 7**).
945   **Sample concentration, C_{mX}:** Normalization for sample concentration is required to
946 report respiratory data. Considering a tissue or cells as the sample, X, the sample mass is m_X
947 [mg], which is frequently measured as wet or dry weight, W_w or W_d [mg], or as amount of tissue
948 or cell protein, $m_{Protein}$. In the case of permeabilized tissues, cells, and homogenates, the sample
949 concentration, $C_{mX} = m_X/V$ [$g \cdot L^{-1} = mg \cdot mL^{-1}$], is the mass of the subsample of tissue that is
950 transferred into the instrument chamber.
951   **Mass-specific flux, $J_{O_2/mX}$:** Mass-specific flux is obtained by expressing respiration per
952 mass of sample, m_X [mg]. X is the type of sample—isolated mitochondria, tissue homogenate,
953 permeabilized fibres or cells. Volume-specific flux is divided by mass concentration of X, $J_{O_2/mX}$
954 $= J_{V,O_2}/C_{mX}$; or flow per cell is divided by mass per cell, $J_{O_2/mcell} = I_{O_2/cell}/M_{cell}$. If mass-specific
955 O_2 flux is constant and independent of sample size (expressed as mass), then there is no
956 interaction between the subsystems. A 1.5 mg and a 3.0 mg muscle sample respires at identical
957 mass-specific flux. Mass-specific O_2 flux, however, may change with the mass of a tissue
958 sample, cells or isolated mitochondria in the measuring chamber, in which the nature of the

959 interaction becomes an issue. Therefore, cell density must be optimization, particularly in
960 experiments carried out in wells, considering the confluency of the cell monolayer or clumps
961 of cells (Salabei *et al.* 2014).
962   **Number concentration, C_{NX}:** C_{NX} is the experimental *number concentration* of sample
963 X. In the case of cells or animals, *e.g.*, nematodes, $C_{NX} = N_X/V$ [x·L^{-1}], where N_X is the number
964 of cells or organisms in the chamber (**Table 4**).
965
966 **Table 4. Sample concentrations and normalization of flux.**

Expression	Symbol	Definition	Unit	Notes
Sample				
identity of sample	X	object: cell, tissue, animal, patient		
number of sample entities X	N_X	number of objects	x	
mass of sample X	m_X		kg	1
mass of object X	M_X	$M_X = m_X \cdot N_X^{-1}$	kg·x^{-1}	1
Mitochondria				
mitochondria	mt	$X = $ mt		
amount of mt-elements	mtE	quantity of mt-marker	mtEU	
Concentrations				
object number concentration	C_{NX}	$C_{NX} = N_X \cdot V^{-1}$	x·m^{-3}	2
sample mass concentration	C_{mX}	$C_{mX} = m_X \cdot V^{-1}$	kg·m^{-3}	
mitochondrial concentration	C_{mtE}	$C_{mtE} = mtE \cdot V^{-1}$	mtEU·m^{-3}	3
specific mitochondrial density	D_{mtE}	$D_{mtE} = mtE \cdot m_X^{-1}$	mtEU·kg^{-1}	4
mitochondrial content, mtE per object X	mtE_X	$mtE_X = mtE \cdot N_X^{-1}$	mtEU·x^{-1}	5
O$_2$ flow and flux				6
flow, system	I_{O_2}	internal flow	mol·s^{-1}	7
volume-specific flux	J_{V,O_2}	$J_{V,O_2} = I_{O_2} \cdot V^{-1}$	mol·s^{-1}·m^{-3}	8
flow per object X	$I_{O_2/X}$	$I_{O_2/X} = J_{V,O_2} \cdot C_{NX}^{-1}$	mol·s^{-1}·x^{-1}	9
mass-specific flux	$J_{O_2/mX}$	$J_{O_2/mX} = J_{V,O_2} \cdot C_{mX}^{-1}$	mol·s^{-1}·kg^{-1}	
mitochondria-specific flux	$J_{O_2/mtE}$	$J_{O_2/mtE} = J_{V,O_2} \cdot C_{mtE}^{-1}$	mol·s^{-1}·mtEU^{-1}	10

967 1   The *SI* prefix k is used for the SI base unit of mass (kg = 1,000 g). In praxis, various *SI* prefixes are
968   used for convenience, to make numbers easily readable, *e.g.,* 1 mg tissue, cell or mitochondrial mass
969   instead of 0.000001 kg.
970 2   In case sample X = cells, the object number concentration is $C_{Ncell} = N_{cell} \cdot V^{-1}$, and volume may be
971   expressed in [dm^3 ≡ L] or [cm^3 = mL]. See **Table 5** for different object types.
972 3   mt-concentration is an experimental variable, dependent on sample concentration: (*1*) $C_{mtE} = mtE \cdot V^{-1}$;
973   (*2*) $C_{mtE} = mtE_X \cdot C_{NX}$; (*3*) $C_{mtE} = C_{mX} \cdot D_{mtE}$.
974 4   If the amount of mitochondria, *mtE*, is expressed as mitochondrial mass, then D_{mtE} is the mass
975   fraction of mitochondria in the sample. If *mtE* is expressed as mitochondrial volume, V_{mt}, and the
976   mass of sample, m_X, is replaced by volume of sample, V_X, then D_{mtE} is the volume fraction of
977   mitochondria in the sample.
978 5 $mtE_X = mtE \cdot N_X^{-1} = C_{mtE} \cdot C_{NX}^{-1}$.
979 6   O$_2$ can be replaced by other chemicals B to study different reactions, *e.g.,* ATP, H$_2$O$_2$, or
980   compartmental translocations, *e.g.,* Ca^{2+}.
981 7 I_{O_2} and V are defined per instrument chamber as a system of constant volume (and constant
982   temperature), which may be closed or open. I_{O_2} is abbreviated for I_{rO_2}, *i.e.*, the metabolic or internal
983   O$_2$ flow of the chemical reaction r in which O$_2$ is consumed, hence the negative stoichiometric
984   number, $v_{O_2} = -1$. $I_{rO_2} = d_r n_{O_2}/dt \cdot v_{O_2}^{-1}$. If r includes all chemical reactions in which O$_2$ participates, then
985     $d_r n_{O_2} = dn_{O_2} - d_e n_{O_2}$, where dn_{O_2} is the change in the amount of O$_2$ in the instrument chamber and $d_e n_{O_2}$

986   is the amount of O_2 added externally to the system. At steady state, by definition $d n_{O_2} = 0$, hence $d_r n_{O_2}$
987       $= -d_e n_{O_2}$.
988   8 J_{V,O_2} is an experimental variable, expressed per volume of the instrument chamber.
989   9 $I_{O_2/X}$ is a physiological variable, depending on the size of entity X.
990   10 There are many ways to normalize for a mitochondrial marker, that are used in different experimental
991   approaches: (1) $J_{O_2/mtE} = J_{V,O_2} \cdot C_{mtE}^{-1}$; (2) $J_{O_2/mtE} = J_{V,O_2} \cdot C_{mX}^{-1} \cdot D_{mtE}^{-1} = J_{O_2/mX} \cdot D_{mtE}^{-1}$; (3) $J_{O_2/mtE} =$
992       $J_{V,O_2} \cdot C_{NX}^{-1} \cdot mtE_X^{-1} = I_{O_2/X} \cdot mtE_X^{-1}$; (4) $J_{O_2/mtE} = I_{O_2} \cdot mtE^{-1}$. The mt-elemental unit [mtEU] varies between
993   different mt-markers.
994   **Table 5. Sample types, *X*, abbreviations, and quantification.**

Identity of sample	X	N_X	Mass[a]	Volume	mt-Marker
mitochondrial preparation	Mtprep	[x]	[kg]	[m^3]	[mtEU]
isolated mitochondria	imt		m_{mt}	V_{mt}	mtE
tissue homogenate	thom		m_{thom}		mtE_{thom}
permeabilized tissue	pti		m_{pti}		mtE_{pti}
permeabilized fibre	pfi		m_{pfi}		mtE_{pfi}
permeabilized cell	pce	N_{pce}	M_{pce}	V_{pce}	mtE_{pce}
intact cell	ce	N_{ce}	M_{ce}	V_{ce}	mtE_{ce}
Organism	org	N_{org}	M_{org}	V_{org}	

995   [a] Instead of mass, frequently the wet weight or dry weight is stated, W_w or W_d.
996   m_X is mass of the sample [kg], M_X is mass of the object [kg·x^{-1}].

997

998   **Flow per object, $I_{O_2/X}$:** A special case of normalization is encountered in respiratory
999 studies with permeabilized (or intact) cells. If respiration is expressed per cell, the O_2 flow per
1000 measurement system is replaced by the O_2 flow per cell, $I_{O_2/cell}$ (**Table 4**). O_2 flow can be
1001 calculated from volume-specific O_2 flux, J_{V,O_2} [nmol·s^{-1}·L^{-1}] (per V of the measurement chamber
1002 [L]), divided by the number concentration of cells, $C_{Nce} = N_{ce}/V$ [cell·L^{-1}], where N_{ce} is the
1003 number of cells in the chamber. Cellular O_2 flow can be compared between cells of identical
1004 size. To take into account changes and differences in cell size, normalization is required to
1005 obtain cell size-specific or mitochondrial marker-specific O_2 flux (Renner *et al.* 2003).
1006   The complexity changes when the sample is a whole organism studied as an experimental
1007 model. The scaling law in respiratory physiology reveals a strong interaction of O_2 consumption
1008 and individual body mass of an organism, since *basal* metabolic rate (flow) does not increase
1009 linearly with body mass, whereas *maximum* mass-specific O_2 flux, $\dot{V}_{O2max}$ or $\dot{V}_{O2peak}$, is
1010 approximately constant across a large range of individual body mass (Weibel and Hoppeler
1011 2005), with individuals, breeds, and species deviating substantially from this relationship.
1012 $\dot{V}_{O2peak}$ of human endurance athletes is 60 to 80 mL O_2·min^{-1}·kg^{-1} body mass, converted to
1013 $J_{M,O2peak}$ of 45 to 60 nmol·s^{-1}·g^{-1} (Gnaiger 2014; **Table 6**).

1014
1015 *3.4. Normalization for mitochondrial content*
1016

1017   Tissues can contain multiple cell populations that may have distinct mitochondrial
1018 subtypes. Mitochondria undergo dynamic fission and fusion cycles, and can exist in multiple
1019 stages and sizes which may be altered by a range of factors. The isolation of mitochondria (often
1020 achieved through differential centrifugation) can therefore yield a subsample of the
1021 mitochondrial types present in a tissue, depending on isolation protocols utilized (*e.g.,*
1022 centrifugation speed). This possible bias should be taken into account when planning
1023 experiments using isolated mitochondria. Different sizes of mitochondria are enriched at
1024 specific centrifugation speeds, which is used for isolation of mitochondrial subpopulations.
1025   Part of the mitochondrial content of a tissue is lost during preparation of isolated
1026 mitochondria. The fraction of mitochondria in the isolate is expressed as mitochondrial
1027 recovery. At a high mitochondrial recovery the sample of isolated mitochondria is more
1028 representative of the total mitochondrial population than in preparations characterized by low

1029 recovery. Determination of the mitochondrial recovery and yield is based on measurement of
1030 the concentration of a mitochondrial marker in the tissue homogenate, $C_{mtE,thom}$, which
1031 simultaneously provides information on the specific mitochondrial density in the sample.
1032   Normalization is a problematic subject; it is essential to consider the question of the study.
1033 If the study aims at comparing tissue performance—such as the effects of a treatment on a
1034 specific tissue, then normalization can be successful, using tissue mass or protein content, for
1035 example. However, if the aim is to find differences on mitochondrial function independent of
1036 mitochondrial density (**Table 4**), then normalization to a mitochondrial marker is imperative
1037 (**Fig. 7**). One cannot assume that quantitative changes in various markers—such as
1038 mitochondrial proteins—necessarily occur in parallel with one another. It should be established
1039 that the marker chosen is not selectively altered by the performed treatment. In conclusion, the
1040 normalization must reflect the question under investigation to reach a satisfying answer. On the
1041 other hand, the goal of comparing results across projects and institutions requires
1042 standardization on normalization for entry into a databank.
1043

1044
1045 **Fig. 7. Structure-function analysis of performance of an organism, organ or tissue, or a**
1046 **cell (sample entity, X). O₂ flow, $I_{O_2/X}$, is the product of performance per functional element**
1047 **(element function, mitochondria-specific flux), element density (mitochondrial density,**
1048 **D_{mtE}), and size of entity X (mass, M_X).** (**A**) Structured analysis: performance is the product of
1049 mitochondrial *function* (mt-specific flux) and *structure* (functional elements; D_{mtE} times mass
1050 of X). (**B**) Unstructured analysis: performance is the product of *entity mass-specific flux*, $J_{O_2/MX}$
1051 $= I_{O_2/X}/M_X = I_{O_2}/m_X$ [mol·s^{-1}·kg^{-1}] and *size of entity*, expressed as mass of X; $M_X = m_X \cdot N_X^{-1}$
1052 [kg·x^{-1}]. See **Table 4** for further explanation of quantities and units. Modified from Gnaiger
1053 (2014).
1054
1055   **Mitochondrial concentration, C_{mtE}, and mitochondrial markers:** Mitochondrial
1056 organelles comprise a dynamic cellular reticulum in various states of fusion and fission. Hence,
1057 the definition of an "amount" of mitochondria is often misconceived: mitochondria cannot be
1058 counted reliably as a number of occurring elements. Therefore, quantification of the "amount"
1059 of mitochondria depends on the measurement of chosen mitochondrial markers. 'Mitochondria
1060 are the structural and functional elemental units of cell respiration' (Gnaiger 2014). The
1061 quantity of a mitochondrial marker can reflect the amount of *mitochondrial elements*, *mtE*,

expressed in various mitochondrial elemental units [mtEU] specific for each measured mt-marker (**Table 4**). However, since mitochondrial quality may change in response to stimuli—particularly in mitochondrial dysfunction and after exercise training (Pesta *et al.* 2011; Campos *et al.* 2017)—some markers can vary while others are unchanged: (*1*) Mitochondrial volume and membrane area are structural markers, whereas mitochondrial protein mass is frequently used as a marker for isolated mitochondria. (*2*) Molecular and enzymatic mitochondrial markers (amounts or activities) can be selected as matrix markers, *e.g.*, citrate synthase activity, mtDNA; mtIM-markers, *e.g.*, cytochrome *c* oxidase activity, aa_3 content, cardiolipin, or mtOM-markers, *e.g.*, TOM20. (*3*) Extending the measurement of mitochondrial marker enzyme activity to mitochondrial pathway capacity, ET- or OXPHOS-capacity can be considered as an integrative functional mitochondrial marker.

Depending on the type of mitochondrial marker, the mitochondrial elements, *mtE*, are expressed in marker-specific units. Mitochondrial concentration in the measurement chamber and the tissue of origin are quantified as (*1*) a quantity for normalization in functional analyses, C_{mtE}, and (*2*) a physiological output that is the result of mitochondrial biogenesis and degradation, D_{mtE}, respectively (**Table 4**). It is recommended, therefore, to distinguish *experimental mitochondrial concentration*, $C_{mtE} = mtE/V$ and *physiological mitochondrial density*, $D_{mtE} = mtE/m_X$. Then mitochondrial density is the amount of mitochondrial elements per mass of tissue, which is a biological variable (**Fig. 7**). The experimental variable is mitochondrial density multiplied by sample mass concentration in the measuring chamber, $C_{mtE} = D_{mtE} \cdot C_{mX}$, or mitochondrial content multiplied by sample number concentration, $C_{mtE} = mtE_X \cdot C_{NX}$ (**Table 4**).

Mitochondria-specific flux, $J_{O_2/mtE}$: Volume-specific metabolic O_2 flux depends on: (*1*) the sample concentration in the volume of the instrument chamber, C_{mX}, or C_{NX}; (*2*) the mitochondrial density in the sample, $D_{mtE} = mtE/m_X$ or $mtE_X = mtE/N_X$; and (*3*) the specific mitochondrial activity or performance per elemental mitochondrial unit, $J_{O_2/mtE} = J_{V,O_2}/C_{mtE}$ [$mol \cdot s^{-1} \cdot mtEU^{-1}$] (**Table 4**). Obviously, the numerical results for $J_{O_2/mtE}$ vary with the type of mitochondrial marker chosen for measurement of *mtE* and $C_{mtE} = mtE/V$ [$mtEU \cdot m^{-3}$].

3.5. Evaluation of mitochondrial markers

Different methods are implicated in the quantification of mitochondrial markers and have different strengths. Some problems are common for all mitochondrial markers, *mtE*: (*1*) Accuracy of measurement is crucial, since even a highly accurate and reproducible measurement of O_2 flux results in an inaccurate and noisy expression normalized for a biased and noisy measurement of a mitochondrial marker. This problem is acute in mitochondrial respiration because the denominators used (the mitochondrial markers) are often small moieties of which accurate and precise determination is difficult. This problem can be avoided when O_2 fluxes measured in substrate-uncoupler-inhibitor titration protocols are normalized for flux in a defined respiratory reference state, which is used as an *internal* marker and yields flux control ratios, *FCR*s. *FCR*s are independent of any *externally* measured markers and, therefore, are statistically robust, considering the limitations of ratios in general (Jasienski and Bazzaz 1999). *FCR*s indicate qualitative changes of mitochondrial respiratory control, with highest quantitative resolution, separating the effect of mitochondrial density or concentration on $J_{O_2/mX}$ and $I_{O_2/X}$ from that of function per elemental mitochondrial marker, $J_{O_2/mtE}$ (Pesta *et al.* 2011; Gnaiger 2014). (*2*) If mitochondrial quality does not change and only the amount of mitochondria varies as a determinant of mass-specific flux, any marker is equally qualified in principle; then in practice selection of the optimum marker depends only on the accuracy and precision of measurement of the mitochondrial marker. (*3*) If mitochondrial flux control ratios change, then there may not be any best mitochondrial marker. In general, measurement of multiple mitochondrial markers enables a comparison and evaluation of normalization for a

1113 variety of mitochondrial markers. Particularly during postnatal development, the activity of
1114 marker enzymes—such as cytochrome *c* oxidase and citrate synthase—follows different time
1115 courses (Drahota *et al.* 2004). Evaluation of mitochondrial markers in healthy controls is
1116 insufficient for providing guidelines for application in the diagnosis of pathological states and
1117 specific treatments.
1118   In line with the concept of the respiratory control ratio (Chance and Williams 1955a), the
1119 most readily used normalization is that of flux control ratios and flux control factors (Gnaiger
1120 2014). Selection of the state of maximum flux in a protocol as the reference state has the
1121 advantages of: (*1*) internal normalization; (*2*) statistical linearization of the response in the range
1122 of 0 to 1; and (*3*) consideration of maximum flux for integrating a large number of elemental
1123 steps in the OXPHOS- or ET-pathways. This reduces the risk of selecting a functional marker
1124 that is specifically altered by the treatment or pathology, yet increases the chance that the highly
1125 integrative pathway is disproportionately affected, *e.g.,* the OXPHOS- rather than ET-pathway
1126 in case of an enzymatic defect in the phosphorylation-pathway. In this case, additional
1127 information can be obtained by reporting flux control ratios based on a reference state which
1128 indicates stable tissue-mass specific flux. Stereological determination of mitochondrial content
1129 via two-dimensional transmission electron microscopy can have limitations due to the dynamics
1130 of mitochondrial size (Meinild Lundby *et al.* 2017). Accurate determination of three-
1131 dimensional volume by two-dimensional microscopy can be both time consuming and
1132 statistically challenging (Larsen *et al.* 2012).
1133   The validity of using mitochondrial marker enzymes (citrate synthase activity, Complex
1134 I–IV amount or activity) for normalization of flux is limited in part by the same factors that
1135 apply to flux control ratios. Strong correlations between various mitochondrial markers and
1136 citrate synthase activity (Reichmann *et al.* 1985; Boushel *et al.* 2007; Mogensen *et al.* 2007)
1137 are expected in a specific tissue of healthy subjects and in disease states not specifically
1138 targeting citrate synthase. Citrate synthase activity is acutely modifiable by exercise
1139 (Tonkonogi *et al.* 1997; Leek *et al.* 2001). Evaluation of mitochondrial markers related to a
1140 selected age and sex cohort cannot be extrapolated to provide recommendations for
1141 normalization in respirometric diagnosis of disease, in different states of development and
1142 ageing, different cell types, tissues, and species. mtDNA normalized to nDNA via qPCR is
1143 correlated to functional mitochondrial markers including OXPHOS- and ET-capacity in some
1144 cases (Puntschart *et al.* 1995; Wang *et al.* 1999; Menshikova *et al.* 2006; Boushel *et al.* 2007),
1145 but lack of such correlations have been reported (Menshikova *et al.* 2005; Schultz and Wiesner
1146 2000; Pesta *et al.* 2011). Several studies indicate a strong correlation between cardiolipin
1147 content and increase in mitochondrial function with exercise (Menshikova *et al.* 2005;
1148 Menshikova *et al.* 2007; Larsen *et al.* 2012; Faber *et al.* 2014), but its use as a general
1149 mitochondrial biomarker in disease remains questionable.
1150
1151 *3.6. Conversion: units*
1152
1153   Many different units have been used to report the rate of oxygen consumption, OCR
1154 (**Table 6**). *SI* base units provide the common reference to introduce the theoretical principles
1155 (**Fig. 6**), and are used with appropriately chosen *SI* prefixes to express numerical data in the
1156 most practical format, with an effort towards unification within specific areas of application
1157 (**Table 7**). Reporting data in *SI* units—including the mole [mol], coulomb [C], joule [J], and
1158 second [s]—should be encouraged, particularly by journals which propose the use of *SI* units.
1159   Although volume is expressed as m^3 using the *SI* base unit, the litre [dm^3] is a
1160 conventional unit of volume for concentration and is used for most solution chemical kinetics.
1161 If one multiplies $I_{O_2/cell}$ by C_{Ncell}, then the result will not only be the amount of O_2 [mol]
1162 consumed per time [s^{-1}] in one litre [L^{-1}], but also the change in the concentration of oxygen per
1163 second (for any volume of an ideally closed system). This is ideal for kinetic modeling as it

1164 blends with chemical rate equations where concentrations are typically expressed in $mol \cdot L^{-1}$
1165 (Wagner *et al.* 2011). In studies of multinuclear cells—such as differentiated skeletal muscle
1166 cells—it is easy to determine the number of nuclei but not the total number of cells. A
1167 generalized concept, therefore, is obtained by substituting cells by nuclei as the sample entity.
1168 This does not hold, however, for enucleated platelets.
1169
1170
1171 **Table 6. Conversion of various units used in respirometry and**
1172 **ergometry.** e^- is the number of electrons or reducing equivalents. z_B is the
1173 charge number of entity B.
1174

1 Unit	x	Multiplication factor	*SI*-unit	Note
$ng.atom\ O \cdot s^{-1}$	$(2\ e^-)$	0.5	$nmol\ O_2 \cdot s^{-1}$	
$ng.atom\ O \cdot min^{-1}$	$(2\ e^-)$	8.33	$pmol\ O_2 \cdot s^{-1}$	
$natom\ O \cdot min^{-1}$	$(2\ e^-)$	8.33	$pmol\ O_2 \cdot s^{-1}$	
$nmol\ O_2 \cdot min^{-1}$	$(4\ e^-)$	16.67	$pmol\ O_2 \cdot s^{-1}$	
$nmol\ O_2 \cdot h^{-1}$	$(4\ e^-)$	0.2778	$pmol\ O_2 \cdot s^{-1}$	
$mL\ O_2 \cdot min^{-1}$ at $STPD^a$		0.744	$\mu mol\ O_2 \cdot s^{-1}$	1
$W = J/s$ at $-470\ kJ/mol\ O_2$		-2.128	$\mu mol\ O_2 \cdot s^{-1}$	
$mA = mC \cdot s^{-1}$	$(z_{H+} = 1)$	10.36	$nmol\ H^+ \cdot s^{-1}$	2
$mA = mC \cdot s^{-1}$	$(z_{O_2} = 4)$	2.59	$nmol\ O_2 \cdot s^{-1}$	2
$nmol\ H^+ \cdot s^{-1}$	$(z_{H+} = 1)$	0.09649	mA	3
$nmol\ O_2 \cdot s^{-1}$	$(z_{O_2} = 4)$	0.38594	mA	3

1175 1 At standard temperature and pressure dry (STPD: 0 °C = 273.15 K and 1 atm =
1176 101.325 kPa = 760 mmHg), the molar volume of an ideal gas, V_m, and V_{m,O_2} is
1177 22.414 and 22.392 $L \cdot mol^{-1}$, respectively. Rounded to three decimal places, both
1178 values yield the conversion factor of 0.744. For comparison at NTPD (20 °C),
1179 V_{m,O_2} is 24.038 $L \cdot mol^{-1}$. Note that the *SI* standard pressure is 100 kPa.
1180 2 The multiplication factor is $10^6/(z_B \cdot F)$.
1181 3 The multiplication factor is $z_B \cdot F/10^6$.
1182
1183

1184   For studies of cells, we recommend that respiration be expressed, as far as possible, as:
1185 (*1*) O_2 flux normalized for a mitochondrial marker, for separation of the effects of mitochondrial
1186 quality and content on cell respiration (this includes *FCR*s as a normalization for a functional
1187 mitochondrial marker); (*2*) O_2 flux in units of cell volume or mass, for comparison of respiration
1188 of cells with different cell size (Renner *et al.* 2003) and with studies on tissue preparations, and
1189 (*3*) O_2 flow in units of attomole (10^{-18} mol) of O_2 consumed in a second by each cell
1190 [$amol \cdot s^{-1} \cdot cell^{-1}$], numerically equivalent to [$pmol \cdot s^{-1} \cdot 10^{-6}$ cells]. This convention allows
1191 information to be easily used when designing experiments in which oxygen consumption must
1192 be considered. For example, to estimate the volume-specific O_2 flux in an instrument chamber
1193 that would be expected at a particular cell number concentration, one simply needs to multiply
1194 the flow per cell by the number of cells per volume of interest. This provides the amount of O_2
1195 [mol] consumed per time [s^{-1}] per unit volume [L^{-1}]. At an O_2 flow of 100 $amol \cdot s^{-1} \cdot cell^{-1}$ and a
1196 cell density of 10^9 $cells \cdot L^{-1}$ (10^6 $cells \cdot mL^{-1}$), the volume-specific O_2 flux is 100 $nmol \cdot s^{-1} \cdot L^{-1}$ (100
1197 $pmol \cdot s^{-1} \cdot mL^{-1}$).
1198   ET-capacity in human cell types including HEK 293, primary HUVEC and fibroblasts
1199 ranges from 50 to 180 $amol \cdot s^{-1} \cdot cell^{-1}$, measured in intact cells in the noncoupled state (see
1200 Gnaiger 2014). At 100 $amol \cdot s^{-1} \cdot cell^{-1}$ corrected for *Rox*, the current across the mt-membranes,

1201 I_{H+e}, approximates 193 pA·cell^{-1} or 0.2 nA per cell. See Rich (2003) for an extension of
1202   quantitative bioenergetics from the molecular to the human scale, with a transmembrane proton
1203   flux equivalent to 520 A in an adult at a catabolic power of -110 W. Modelling approaches
1204   illustrate the link between protonmotive force and currents (Willis *et al.* 2016).

1205
1206

1207   **Table 7. Conversion of units with preservation of numerical values.**

Name	Frequently used unit	Equivalent unit	Note
volume-specific flux, J_{V,O_2}	pmol·s^{-1}·mL^{-1}	nmol·s^{-1}·L^{-1}	1
	mmol·s^{-1}·L^{-1}	mol·s^{-1}·m^{-3}	
cell-specific flow, $I_{O_2/cell}$	pmol·s^{-1}·10^{-6} cells	amol·s^{-1}·cell^{-1}	2
	pmol·s^{-1}·10^{-9} cells	zmol·s^{-1}·cell^{-1}	3
cell number concentration, C_{Nce}	10^6 cells·mL^{-1}	10^9 cells·L^{-1}	
mitochondrial protein concentration, C_{mtE}	0.1 mg·mL^{-1}	0.1 g·L^{-1}	
mass-specific flux, $J_{O_2/m}$	pmol·s^{-1}·mg^{-1}	nmol·s^{-1}·g^{-1}	4
catabolic power, P_k	µW·10^{-6} cells	pW·cell^{-1}	1
Volume	1,000 L	m^3 (1,000 kg)	
	L	dm^3 (kg)	
	mL	cm^3 (g)	
	µL	mm^3 (mg)	
	fL	µm^3 (pg)	5
amount of substance concentration	M = mol·L^{-1}	mol·dm^{-3}	

1208
1209   1   pmol: picomole = 10^{-12} mol   4   nmol: nanomole = 10^{-9} mol
1210   2   amol: attomole = 10^{-18} mol   5   fL: femtolitre = 10^{-15} L
1211   3   zmol: zeptomole = 10^{-21} mol
1212
1213

1214   We consider isolated mitochondria as powerhouses and proton pumps as molecular
1215 machines to relate experimental results to energy metabolism of the intact cell. The cellular
1216 P»/O$_2$ based on oxidation of glycogen is increased by the glycolytic (fermentative) substrate-
1217 level phosphorylation of 3 P»/Glyc or 0.5 mol P» for each mol O$_2$ consumed in the complete
1218 oxidation of a mol glycosyl unit (Glyc). Adding 0.5 to the mitochondrial P»/O$_2$ ratio of 5.4
1219 yields a bioenergetic cell physiological P»/O$_2$ ratio close to 6. Two NADH equivalents are
1220 formed during glycolysis and transported from the cytosol into the mitochondrial matrix, either
1221 by the malate-aspartate shuttle or by the glycerophosphate shuttle resulting in different
1222 theoretical yields of ATP generated by mitochondria, the energetic cost of which potentially
1223 must be taken into account. Considering also substrate-level phosphorylation in the TCA cycle,
1224 this high P»/O$_2$ ratio not only reflects proton translocation and OXPHOS studied in isolation,
1225 but integrates mitochondrial physiology with energy transformation in the living cell (Gnaiger
1226 1993a).

1227
1228

1229 **4. Conclusions**

1230

1231   MitoEAGLE can serve as a gateway to better diagnose mitochondrial respiratory defects
1232 linked to genetic variation, age-related health risks, sex-specific mitochondrial performance,
1233 lifestyle with its effects on degenerative diseases, and thermal and chemical environment. The
1234 present recommendations on coupling control states and rates, linked to the concept of the

protonmotive force, are focused on studies with mitochondrial preparations. These will be extended in a series of reports on pathway control of mitochondrial respiration, respiratory states in intact cells, and harmonization of experimental procedures.

The optimal choice for expressing mitochondrial and cell respiration (**Box 3**) as O_2 flow per biological system, and normalization for specific tissue-markers (volume, mass, protein) and mitochondrial markers (volume, protein, content, mtDNA, activity of marker enzymes, respiratory reference state) is guided by the scientific question under study. Interpretation of the obtained data depends critically on appropriate normalization, and therefore reporting rates merely as $nmol·s^{-1}$ is discouraged, since it restricts the analysis to intra-experimental comparison of relative (qualitative) differences. Expressing O_2 consumption per cell may not be possible when dealing with tissues. For studies with mitochondrial preparations, we recommend that normalizations be provided as far as possible: (*1*) on a per cell basis as O_2 flow (a biophysical normalization); (*2*) per g cell or tissue protein, or per cell or tissue mass as mass-specific O_2 flux (a cellular normalization); and (*3*) per mitochondrial marker as mt-specific flux (a mitochondrial normalization). With information on cell size and the use of multiple normalizations, maximum potential information is available (Renner *et al.* 2003; Wagner *et al.* 2011; Gnaiger 2014).

Total mitochondrial protein is frequently applied as a mitochondrial marker restricted to isolated mitochondria. The mitochondrial recovery and yield, and experimental criteria for evaluation of purity versus integrity should be reported. Mitochondrial markers—such as citrate synthase activity as an enzymatic matrix marker—provide a link to the tissue of origin on the basis of calculating the mitochondrial recovery, *i.e.*, the fraction of mitochondrial marker obtained from a unit mass of tissue.

Box 3: Mitochondrial and cell respiration

Mitochondrial and cell respiration is the process of exergonic and exothermic energy transformation in which scalar redox reactions are coupled to vectorial ion translocation across a semipermeable membrane, which separates the small volume of a bacterial cell or mitochondrion from the larger volume of its surroundings. The electrochemical exergy can be partially conserved in the phosphorylation of ADP to ATP or in ion pumping, or dissipated in an electrochemical short-circuit. Respiration is thus clearly distinguished from fermentation as the counterpart of cellular core energy metabolism. Respiration is separated in mitochondrial preparations from the partial contribution of fermentative pathways of the intact cell. Residual oxygen consumption—as measured after inhibition of mitochondrial electron transfer—does not belong to the class of catabolic reactions and is, therefore, subtracted from total oxygen consumption to obtain baseline-corrected respiration.

Terms and symbols are summarized in **Table 8**. Their use will facilitate transdisciplinary communication and support further developments towards a consistent theory of bioenergetics and mitochondrial physiology. Technical terms related to and defined with normal words can be used as index terms in databases, support the creation of ontologies towards semantic information processing (MitoPedia), and help in communicating analytical findings as impactful data-driven stories. '*Making data available without making it understandable may be worse than not making it available at all*' (National Academies of Sciences, Engineering, and Medicine 2018). This is a call to carefully contribute to FAIR principles (Findable, Accessible, Interoperable, Reusable) for the sharing of scientific data.

Table 8. Terms, symbols, and units.

Term	Symbol	Unit	Links and comments
alternative quinol oxidase	AOX		Fig. 1
amount of substance B	n_B	[mol]	
Complexes I to IV	CI to CIV		respiratory ET Complexes; Fig. 1
concentration of substance B	$c_B = n_B \cdot V^{-1}$; [B]	[mol·m^{-3}]	Box 2
electron transfer system	ETS		Fig. 1, Fig. 4
flow, for substance B	I_B	[mol·s^{-1}]	system-related extensive quantity; Fig. 6
flux, for substance B	J_B	*varies*	size-specific quantitiy; Fig. 6
inorganic phosphate	P_i		Fig. 2
LEAK	LEAK		Tab. 1, Fig. 4
mass of sample X	m_X	[kg]	Tab. 4
mass of entity X	M_X	[kg]	mass of object X; Tab. 4
MITOCARTA			https://www.broadinstitute.org/scientific-community/science/programs/metabolic-disease-program/publications/mitocarta/mitocarta-in-0
MitoPedia			http://www.bioblast.at/index.php/MitoPedia
mitochondria or mitochondrial	mt		Box 1
mitochondrial DNA	mtDNA		Box 1
mitochondrial concentration	$C_{mtE} = mtE \cdot V^{-1}$	[mtEU·m^{-3}]	Tab. 4
mitochondrial content	$mtE_X = mtE \cdot N_X^{-1}$	[mtEU·x^{-1}]	Tab. 4
mitochondrial elemental unit	mtEU	*varies*	Tab. 4, specific units for mt-marker
mitochondrial inner membrane	mtIM		MIM is widely used; the first M is replaced by mt; Box 1
mitochondrial outer membrane	mtOM		MOM is widely used; the first M is replaced by mt; Box 1
mitochondrial recovery	Y_{mtE}		fraction of mtE recovered in sample from the tissue of origin
mitochondrial yield	$Y_{mtE/m}$		$Y_{mtE/m} = Y_{mtE} \cdot D_{mtE}$
negative	neg		Fig. 2
number concentration of X	C_{NX}	[x·m^{-3}]	Tab. 4
number of entities X	N_X	[x]	Tab. 4, Fig. 7
number of entity B	N_B	[x]	Tab. 4
oxidative phosphorylation	OXPHOS		Tab. 1, Fig. 4
oxygen concentration	$c_{O2} = n_{O2} \cdot V^{-1}$; [O$_2$]	[mol·m^{-3}]	Section 3.2
phosphorylation of ADP to ATP	P»		Section 2.2
positive	pos		Fig. 2
proton in the negative compartment	H$^+_{neg}$		Fig. 2
proton in the positive compartment	H$^+_{pos}$		Fig. 2
rate of electron transfer in ET state	E		ET-capacity; Tab. 1
rate of LEAK respiration	L		Tab. 1
rate of oxidative phosphorylation	P		OXPHOS capacity; Tab. 1
rate of residual oxygen consumption	Rox		Tab. 1
residual oxygen consumption	ROX		Tab. 1
specific mitochondrial density	$D_{mtE} = mtE \cdot m_X^{-1}$	[mtEU·kg^{-1}]	Tab. 7
volume	V	[m^{-3}]	
weight, dry weight	W_d	[kg]	used as mass of sample X; Fig. 6
weight, wet weight	W_w	[kg]	used as mass of sample X; Fig. 6

1349
1350

5. References

1351
1352

1353 Altmann R (1894) Die Elementarorganismen und ihre Beziehungen zu den Zellen. Zweite vermehrte Auflage.
1354   Verlag Von Veit & Comp, Leipzig:160 pp.
1355 Beard DA (2005) A biophysical model of the mitochondrial respiratory system and oxidative phosphorylation.
1356   PLoS Comput Biol 1(4):e36.
1357 Benda C (1898) Weitere Mitteilungen über die Mitochondria. Verh Dtsch Physiol Ges:376-83.
1358 Birkedal R, Laasmaa M, Vendelin M (2014) The location of energetic compartments affects energetic
1359   communication in cardiomyocytes. Front Physiol 5:376.
1360 Breton S, Beaupré HD, Stewart DT, Hoeh WR, Blier PU (2007) The unusual system of doubly uniparental
1361   inheritance of mtDNA: isn't one enough? Trends Genet 23:465-74.
1362 Brown GC (1992) Control of respiration and ATP synthesis in mammalian mitochondria and cells. Biochem J
1363   284:1-13.
1364 Calvo SE, Klauser CR, Mootha VK (2016) MitoCarta2.0: an updated inventory of mammalian mitochondrial
1365   proteins. Nucleic Acids Research 44:D1251-7.
1366 Calvo SE, Julien O, Clauser KR, Shen H, Kamer KJ, Wells JA, Mootha VK (2017) Comparative analysis of
1367   mitochondrial N-termini from mouse, human, and yeast. Mol Cell Proteomics 16:512-23.
1368 Campos JC, Queliconi BB, Bozi LHM, Bechara LRG, Dourado PMM, Andres AM, Jannig PR, Gomes KMS,
1369   Zambelli VO, Rocha-Resende C, Guatimosim S, Brum PC, Mochly-Rosen D, Gottlieb RA, Kowaltowski AJ,
1370   Ferreira JCB (2017) Exercise reestablishes autophagic flux and mitochondrial quality control in heart failure.
1371   Autophagy 13:1304-317.
1372 Canton M, Luvisetto S, Schmehl I, Azzone GF (1995) The nature of mitochondrial respiration and
1373   discrimination between membrane and pump properties. Biochem J 310:477-81.
1374 Chance B, Williams GR (1955a) Respiratory enzymes in oxidative phosphorylation. I. Kinetics of oxygen
1375   utilization. J Biol Chem 217:383-93.
1376 Chance B, Williams GR (1955b) Respiratory enzymes in oxidative phosphorylation: III. The steady state. J Biol
1377   Chem 217:409-27.
1378 Chance B, Williams GR (1955c) Respiratory enzymes in oxidative phosphorylation. IV. The respiratory chain. J
1379   Biol Chem 217:429-38.
1380 Chance B, Williams GR (1956) The respiratory chain and oxidative phosphorylation. Adv Enzymol Relat Subj
1381   Biochem 17:65-134.
1382 Cobb LJ, Lee C, Xiao J, Yen K, Wong RG, Nakamura HK, Mehta HH, Gao Q, Ashur C, Huffman DM, Wan J,
1383   Muzumdar R, Barzilai N, Cohen P (2016) Naturally occurring mitochondrial-derived peptides are age-
1384   dependent regulators of apoptosis, insulin sensitivity, and inflammatory markers. Aging (Albany NY) 8:796-
1385   809.
1386 Cohen ER, Cvitas T, Frey JG, Holmström B, Kuchitsu K, Marquardt R, Mills I, Pavese F, Quack M, Stohner J,
1387   Strauss HL, Takami M, Thor HL (2008) Quantities, units and smbols in physical chemistry, IUPAC Green
1388   Book, 3rd Edition, 2nd Printing, IUPAC & RSC Publishing, Cambridge.
1389 Cooper H, Hedges LV, Valentine JC, eds (2009) The handbook of research synthesis and meta-analysis. Russell
1390   Sage Foundation.
1391 Coopersmith J (2010) Energy, the subtle concept. The discovery of Feynman's blocks from Leibnitz to Einstein.
1392   Oxford University Press:400 pp.
1393 Cummins J (1998) Mitochondrial DNA in mammalian reproduction. Rev Reprod 3:172-82.
1394 Dai Q, Shah AA, Garde RV, Yonish BA, Zhang L, Medvitz NA, Miller SE, Hansen EL, Dunn CN, Price TM
1395   (2013) A truncated progesterone receptor (PR-M) localizes to the mitochondrion and controls cellular
1396   respiration. Mol Endocrinol 27:741-53.
1397 Divakaruni AS, Brand MD (2011) The regulation and physiology of mitochondrial proton leak. Physiology
1398   (Bethesda) 26:192-205.
1399 Doerrier C, Garcia-Souza LF, Krumschnabel G, Wohlfarter Y, Mészáros AT, Gnaiger E (2018) High-Resolution
1400   FluoRespirometry and OXPHOS protocols for human cells, permeabilized fibres from small biopsies of
1401   muscle and isolated mitochondria. Methods Mol. Biol. (in press)
1402 Doskey CM, van 't Erve TJ, Wagner BA, Buettner GR (2015) Moles of a substance per cell is a highly
1403   informative dosing metric in cell culture. PLOS ONE 10:e0132572.
1404 Drahota Z, Milerová M, Stieglerová A, Houstek J, Ostádal B (2004) Developmental changes of cytochrome *c*
1405   oxidase and citrate synthase in rat heart homogenate. Physiol Res 53:119-22.
1406 Duarte FV, Palmeira CM, Rolo AP (2014) The role of microRNAs in mitochondria: small players acting wide.
1407   Genes (Basel) 5:865-86.

1408 Ernster L, Schatz G (1981) Mitochondria: a historical review. J Cell Biol 91:227s-55s.
1409 Estabrook RW (1967) Mitochondrial respiratory control and the polarographic measurement of ADP:O ratios.
1410   Methods Enzymol 10:41-7.
1411 Faber C, Zhu ZJ, Castellino S, Wagner DS, Brown RH, Peterson RA, Gates L, Barton J, Bickett M, Hagerty L,
1412   Kimbrough C, Sola M, Bailey D, Jordan H, Elangbam CS (2014) Cardiolipin profiles as a potential
1413   biomarker of mitochondrial health in diet-induced obese mice subjected to exercise, diet-restriction and
1414   ephedrine treatment. J Appl Toxicol 34:1122-9.
1415 Fell D (1997) Understanding the control of metabolism. Portland Press.
1416 Garlid KD, Beavis AD, Ratkje SK (1989) On the nature of ion leaks in energy-transducing membranes. Biochim
1417   Biophys Acta 976:109-20.
1418 Garlid KD, Semrad C, Zinchenko V. Does redox slip contribute significantly to mitochondrial respiration? In:
1419   Schuster S, Rigoulet M, Ouhabi R, Mazat J-P, eds (1993) Modern trends in biothermokinetics. Plenum Press,
1420   New York, London:287-93.
1421 Gerö D, Szabo C (2016) Glucocorticoids suppress mitochondrial oxidant production via upregulation of
1422   uncoupling protein 2 in hyperglycemic endothelial cells. PLoS One 11:e0154813.
1423 Gnaiger E. Efficiency and power strategies under hypoxia. Is low efficiency at high glycolytic ATP production a
1424   paradox? In: Surviving Hypoxia: Mechanisms of Control and Adaptation. Hochachka PW, Lutz PL, Sick T,
1425   Rosenthal M, Van den Thillart G, eds (1993a) CRC Press, Boca Raton, Ann Arbor, London, Tokyo:77-109.
1426 Gnaiger E (1993b) Nonequilibrium thermodynamics of energy transformations. Pure Appl Chem 65:1983-2002.
1427 Gnaiger E (2001) Bioenergetics at low oxygen: dependence of respiration and phosphorylation on oxygen and
1428   adenosine diphosphate supply. Respir Physiol 128:277-97.
1429 Gnaiger E (2009) Capacity of oxidative phosphorylation in human skeletal muscle. New perspectives of
1430   mitochondrial physiology. Int J Biochem Cell Biol 41:1837-45.
1431 Gnaiger E (2014) Mitochondrial pathways and respiratory control. An introduction to OXPHOS analysis. 4th ed.
1432   Mitochondr Physiol Network 19.12. Oroboros MiPNet Publications, Innsbruck:80 pp.
1433 Gnaiger E, Méndez G, Hand SC (2000) High phosphorylation efficiency and depression of uncoupled respiration
1434   in mitochondria under hypoxia. Proc Natl Acad Sci USA 97:11080-5.
1435 Greggio C, Jha P, Kulkarni SS, Lagarrigue S, Broskey NT, Boutant M, Wang X, Conde Alonso S, Ofori E,
1436   Auwerx J, Cantó C, Amati F (2017) Enhanced respiratory chain supercomplex formation in response to
1437   exercise in human skeletal muscle. Cell Metab 25:301-11.
1438 Hinkle PC (2005) P/O ratios of mitochondrial oxidative phosphorylation. Biochim Biophys Acta 1706:1-11.
1439 Hofstadter DR (1979) Gödel, Escher, Bach: An eternal golden braid. A metaphorical fugue on minds and
1440   machines in the spirit of Lewis Carroll. Harvester Press:499 pp.
1441 Illaste A, Laasmaa M, Peterson P, Vendelin M (2012) Analysis of molecular movement reveals latticelike
1442   obstructions to diffusion in heart muscle cells. Biophys J 102:739-48.
1443 Jasienski M, Bazzaz FA (1999) The fallacy of ratios and the testability of models in biology. Oikos 84:321-26.
1444 Jepihhina N, Beraud N, Sepp M, Birkedal R, Vendelin M (2011) Permeabilized rat cardiomyocyte response
1445   demonstrates intracellular origin of diffusion obstacles. Biophys J 101:2112-21.
1446 Klepinin A, Ounpuu L, Guzun R, Chekulayev V, Timohhina N, Tepp K, Shevchuk I, Schlattner U, Kaambre T
1447   (2016) Simple oxygraphic analysis for the presence of adenylate kinase 1 and 2 in normal and tumor cells. J
1448   Bioenerg Biomembr 48:531-48.
1449 Klingenberg M (2017) UCP1 - A sophisticated energy valve. Biochimie 134:19-27.
1450 Koit A, Shevchuk I, Ounpuu L, Klepinin A, Chekulayev V, Timohhina N, Tepp K, Puurand M,Truu L, Heck K,
1451   Valvere V, Guzun R, Kaambre T (2017) Mitochondrial respiration in human colorectal and breast cancer
1452   clinical material is regulated differently. Oxid Med Cell Longev 1372640.
1453 Komlódi T, Tretter L (2017) Methylene blue stimulates substrate-level phosphorylation catalysed by succinyl-
1454   CoA ligase in the citric acid cycle. Neuropharmacology 123:287-98.
1455 Lane N (2005) Power, sex, suicide: mitochondria and the meaning of life. Oxford University Press:354 pp.
1456 Larsen S, Nielsen J, Neigaard Nielsen C, Nielsen LB, Wibrand F, Stride N, Schroder HD, Boushel RC, Helge
1457   JW, Dela F, Hey-Mogensen M (2012) Biomarkers of mitochondrial content in skeletal muscle of healthy
1458   young human subjects. J Physiol 590:3349-60.
1459 Lee C, Zeng J, Drew BG, Sallam T, Martin-Montalvo A, Wan J, Kim SJ, Mehta H, Hevener AL, de Cabo R,
1460   Cohen P (2015) The mitochondrial-derived peptide MOTS-c promotes metabolic homeostasis and reduces
1461   obesity and insulin resistance. Cell Metab 21:443-54.
1462 Lee SR, Kim HK, Song IS, Youm J, Dizon LA, Jeong SH, Ko TH, Heo HJ, Ko KS, Rhee BD, Kim N, Han J
1463   (2013) Glucocorticoids and their receptors: insights into specific roles in mitochondria. Prog Biophys Mol
1464   Biol 112:44-54.
1465 Leek BT, Mudaliar SR, Henry R, Mathieu-Costello O, Richardson RS (2001) Effect of acute exercise on citrate
1466   synthase activity in untrained and trained human skeletal muscle. Am J Physiol Regul Integr Comp Physiol
1467   280:R441-7.
1468 Lemieux H, Blier PU, Gnaiger E (2017) Remodeling pathway control of mitochondrial respiratory capacity by
1469   temperature in mouse heart: electron flow through the Q-junction in permeabilized fibers. Sci Rep 7:2840.

Lenaz G, Tioli G, Falasca AI, Genova ML (2017) Respiratory supercomplexes in mitochondria. In: Mechanisms of primary energy trasduction in biology. M Wikstrom (ed) Royal Society of Chemistry Publishing, London, UK:296-337.

Margulis L (1970) Origin of eukaryotic cells. New Haven: Yale University Press.

Meinild Lundby AK, Jacobs RA, Gehrig S, de Leur J, Hauser M, Bonne TC, Flück D, Dandanell S, Kirk N, Kaech A, Ziegler U, Larsen S, Lundby C (2018) Exercise training increases skeletal muscle mitochondrial volume density by enlargement of existing mitochondria and not de novo biogenesis. Acta Physiol 222, e12905.

Menshikova EV, Ritov VB, Fairfull L, Ferrell RE, Kelley DE, Goodpaster BH (2006) Effects of exercise on mitochondrial content and function in aging human skeletal muscle. J Gerontol A Biol Sci Med Sci 61:534-40.

Menshikova EV, Ritov VB, Ferrell RE, Azuma K, Goodpaster BH, Kelley DE (2007) Characteristics of skeletal muscle mitochondrial biogenesis induced by moderate-intensity exercise and weight loss in obesity. J Appl Physiol (1985) 103:21-7.

Menshikova EV, Ritov VB, Toledo FG, Ferrell RE, Goodpaster BH, Kelley DE (2005) Effects of weight loss and physical activity on skeletal muscle mitochondrial function in obesity. Am J Physiol Endocrinol Metab 288:E818-25.

Miller GA (1991) The science of words. Scientific American Library New York:276 pp.

Mitchell P (1961) Coupling of phosphorylation to electron and hydrogen transfer by a chemi-osmotic type of mechanism. Nature 191:144-8.

Mitchell P (2011) Chemiosmotic coupling in oxidative and photosynthetic phosphorylation. Biochim Biophys Acta Bioenergetics 1807:1507-38.

Mogensen M, Sahlin K, Fernström M, Glintborg D, Vind BF, Beck-Nielsen H, Højlund K (2007) Mitochondrial respiration is decreased in skeletal muscle of patients with type 2 diabetes. Diabetes 56:1592-9.

Mohr PJ, Phillips WD (2015) Dimensionless units in the SI. Metrologia 52:40-7.

Moreno M, Giacco A, Di Munno C, Goglia F (2017) Direct and rapid effects of 3,5-diiodo-L-thyronine (T2). Mol Cell Endocrinol 7207:30092-8.

Morrow RM, Picard M, Derbeneva O, Leipzig J, McManus MJ, Gouspillou G, Barbat-Artigas S, Dos Santos C, Hepple RT, Murdock DG, Wallace DC (2017) Mitochondrial energy deficiency leads to hyperproliferation of skeletal muscle mitochondria and enhanced insulin sensitivity. Proc Natl Acad Sci U S A 114:2705-10.

Murley A, Nunnari J (2016) The emerging network of mitochondria-organelle contacts. Mol Cell 61:648-53.

National Academies of Sciences, Engineering, and Medicine (2018) International coordination for science data infrastructure: Proceedings of a workshop—in brief. Washington, DC: The National Academies Press. doi: https://doi.org/10.17226/25015.

Paradies G, Paradies V, De Benedictis V, Ruggiero FM, Petrosillo G (2014) Functional role of cardiolipin in mitochondrial bioenergetics. Biochim Biophys Acta 1837:408-17.

Pesta D, Gnaiger E (2012) High-Resolution Respirometry. OXPHOS protocols for human cells and permeabilized fibres from small biopsies of human muscle. Methods Mol Biol 810:25-58.

Pesta D, Hoppel F, Macek C, Messner H, Faulhaber M, Kobel C, Parson W, Burtscher M, Schocke M, Gnaiger E (2011) Similar qualitative and quantitative changes of mitochondrial respiration following strength and endurance training in normoxia and hypoxia in sedentary humans. Am J Physiol Regul Integr Comp Physiol 301:R1078–87.

Price TM, Dai Q (2015) The role of a mitochondrial progesterone receptor (PR-M) in progesterone action. Semin Reprod Med 33:185-94.

Puchowicz MA, Varnes ME, Cohen BH, Friedman NR, Kerr DS, Hoppel CL (2004) Oxidative phosphorylation analysis: assessing the integrated functional activity of human skeletal muscle mitochondria – case studies. Mitochondrion 4:377-85. Puntschart A, Claassen H, Jostarndt K, Hoppeler H, Billeter R (1995) mRNAs of enzymes involved in energy metabolism and mtDNA are increased in endurance-trained athletes. Am J Physiol 269:C619-25.

Quiros PM, Mottis A, Auwerx J (2016) Mitonuclear communication in homeostasis and stress. Nat Rev Mol Cell Biol 17:213-26.

Reichmann H, Hoppeler H, Mathieu-Costello O, von Bergen F, Pette D (1985) Biochemical and ultrastructural changes of skeletal muscle mitochondria after chronic electrical stimulation in rabbits. Pflugers Arch 404:1-9.

Renner K, Amberger A, Konwalinka G, Gnaiger E (2003) Changes of mitochondrial respiration, mitochondrial content and cell size after induction of apoptosis in leukemia cells. Biochim Biophys Acta 1642:115-23.

Rich P (2003) Chemiosmotic coupling: The cost of living. Nature 421:583.

Rostovtseva TK, Sheldon KL, Hassanzadeh E, Monge C, Saks V, Bezrukov SM, Sackett DL (2008) Tubulin binding blocks mitochondrial voltage-dependent anion channel and regulates respiration. Proc Natl Acad Sci USA 105:18746-51.

Rustin P, Parfait B, Chretien D, Bourgeron T, Djouadi F, Bastin J, Rötig A, Munnich A (1996) Fluxes of nicotinamide adenine dinucleotides through mitochondrial membranes in human cultured cells. J Biol Chem 271:14785-90.

Saks VA, Veksler VI, Kuznetsov AV, Kay L, Sikk P, Tiivel T, Tranqui L, Olivares J, Winkler K, Wiedemann F, Kunz WS (1998) Permeabilised cell and skinned fiber techniques in studies of mitochondrial function in vivo. Mol Cell Biochem 184:81-100.

Salabei JK, Gibb AA, Hill BG (2014) Comprehensive measurement of respiratory activity in permeabilized cells using extracellular flux analysis. Nat Protoc 9:421-38.

Sazanov LA (2015) A giant molecular proton pump: structure and mechanism of respiratory complex I. Nat Rev Mol Cell Biol 16:375-88.

Schneider TD (2006) Claude Shannon: biologist. The founder of information theory used biology to formulate the channel capacity. IEEE Eng Med Biol Mag 25:30-3.

Schönfeld P, Dymkowska D, Wojtczak L (2009) Acyl-CoA-induced generation of reactive oxygen species in mitochondrial preparations is due to the presence of peroxisomes. Free Radic Biol Med 47:503-9.

Schultz J, Wiesner RJ (2000) Proliferation of mitochondria in chronically stimulated rabbit skeletal muscle--transcription of mitochondrial genes and copy number of mitochondrial DNA. J Bioenerg Biomembr 32:627-34.

Simson P, Jepihhina N, Laasmaa M, Peterson P, Birkedal R, Vendelin M (2016) Restricted ADP movement in cardiomyocytes: Cytosolic diffusion obstacles are complemented with a small number of open mitochondrial voltage-dependent anion channels. J Mol Cell Cardiol 97:197-203.

Stucki JW, Ineichen EA (1974) Energy dissipation by calcium recycling and the efficiency of calcium transport in rat-liver mitochondria. Eur J Biochem 48:365-75.

Tonkonogi M, Harris B, Sahlin K (1997) Increased activity of citrate synthase in human skeletal muscle after a single bout of prolonged exercise. Acta Physiol Scand 161:435-6.

Waczulikova I, Habodaszova D, Cagalinec M, Ferko M, Ulicna O, Mateasik A, Sikurova L, Ziegelhöffer A (2007) Mitochondrial membrane fluidity, potential, and calcium transients in the myocardium from acute diabetic rats. Can J Physiol Pharmacol 85:372-81.

Wagner BA, Venkataraman S, Buettner GR (2011) The rate of oxygen utilization by cells. Free Radic Biol Med 51:700-712.

Wang H, Hiatt WR, Barstow TJ, Brass EP (1999) Relationships between muscle mitochondrial DNA content, mitochondrial enzyme activity and oxidative capacity in man: alterations with disease. Eur J Appl Physiol Occup Physiol 80:22-7.

Watt IN, Montgomery MG, Runswick MJ, Leslie AG, Walker JE (2010) Bioenergetic cost of making an adenosine triphosphate molecule in animal mitochondria. Proc Natl Acad Sci U S A 107:16823-7.

Weibel ER, Hoppeler H (2005) Exercise-induced maximal metabolic rate scales with muscle aerobic capacity. J Exp Biol 208:1635–44.

White DJ, Wolff JN, Pierson M, Gemmell NJ (2008) Revealing the hidden complexities of mtDNA inheritance. Mol Ecol 17:4925–42.

Wikström M, Hummer G (2012) Stoichiometry of proton translocation by respiratory complex I and its mechanistic implications. Proc Natl Acad Sci U S A 109:4431-6.

Willis WT, Jackman MR, Messer JI, Kuzmiak-Glancy S, Glancy B (2016) A simple hydraulic analog model of oxidative phosphorylation. Med Sci Sports Exerc 48:990-1000.